Differential osmotic pressure measurements of the concentration susceptibility of liquid ^{3}He/^{4}He mixtures near the lambda curve and tricritical point

C. A. Gearhart, Jr.* and W. Zimmermann, Jr.
Tate Laboratory of Physics, University of Minnesota
Minneapolis, Minnesota 55455
(Received 13 November 1978)

Values of the concentration susceptibility $(\partial x/\partial\Delta)_{T,P}$ of liquid ^{3}He/^{4}He mixtures have been determined near the lambda curve and tricritical point from measurements of the differential osmotic pressure as a function of temperature T at four values of the ^{3}He mole fraction, $x=0.594$, $x=0.644$, $x=0.680$, and $x=0.706$. Here $\Delta=\mu_3-\mu_4$ is the difference between molar chemical potentials and P is the pressure. Our results for the two values of x less than the tricritical value $x_t=0.675$ show pronounced peaks at the lambda transition. For $3\times10^{-4}\lesssim|t|\lesssim10^{-2}$, where t equals $[T-T_\lambda(x)]/T_\lambda(x)$, these peaks may be characterized both above and below the transition by the form $(A_\pm/\alpha_\pm)(|t|^{-\alpha_\pm}-1)+B_\pm$, with exponents $\alpha_\pm$ lying in the range from ~0.0 to ~0.2. Except perhaps for $x<x_t$ in the normal-fluid region away from the lambda transition, our data appear to be consistent with a simple tricritical scaling relationship of the form

$$\left(\frac{\partial x}{\partial\Delta}\right)_{T,P}=f(x)\Xi^{-1}\left[\left(\frac{T-T_t}{T_t}\right)\Big/\left|\frac{x-x_t}{x_t}\right|\right],$$

where f and Ξ are functions determined by experiment and $T_t=0.867$ K is the tricritical value of T. With the aid of this scaling relationship, the behavior of $(\partial x/\partial\Delta)_{T,P}$ along curves of constant Δ near the lambda curve has been constructed from our data at constant x.

I. INTRODUCTION

Tricritical points have recently attracted much experimental and theoretical interest.[1] The tricritical point in ^{3}He/^{4}He mixtures is a particularly suitable one for study, in view of the ease of obtaining pure and homogeneous samples. Experiments on the thermodynamic behavior of the mixtures near the tricritical point include capacitance[2,3] and optical[4,5] measurements of the density along the two branches of the phase-separation curve, optical measurements of the interfacial tension between the phases coexisting along those branches,[5,6] measurements of the molar specific heat $c_{P,x}$ at constant pressure P and ^{3}He mole fraction x,[7,8] second-sound measurements of the superfluid density,[9] capacitance measurements of the gravitational variation of x with height at various pressures,[10] and measurements of the concentration susceptibility $(\partial x/\partial\Delta)_{T,P}$ by means of vapor pressure,[11,12] light-scattering,[4,13] and capacitive gravitational concentration gradient[14,15,16] measurements. Here Δ is the difference $\mu_3-\mu_4$ between molar chemical potentials and T is the absolute temperature. In addition, several experiments have been performed which deal with dynamic effects near the tricritical point.[17–20]

The quantity $(\partial x/\partial\Delta)_{T,P}$ is analogous in T,Δ space (at constant P) to the quantity $(\partial v/\partial P)_T$, where v is the molar volume, for a pure fluid in T,P space. It is of particular importance because of the information that it contains about the relation between the variables T, x, and Δ. We report here determinations of $(\partial x/\partial\Delta)_{T,P}$ from measurements of the differential osmotic pressure at saturated vapor pressure. The range of these measurements is shown by the vertical lines in the phase diagram of Fig. 1. We have been especially interested in the lambda transition, where, contrary to the vapor-pressure and light-scattering results, our data show a pronounced peak. The recent gravitational concentration gradient results confirm the existence of this peak.[15,16] A more detailed account of our work than is presented in this paper may be found in the Ph.D. thesis of one of us (C.A.G.).[21]

The thermodynamics underlying our determination of $(\partial x/\partial\Delta)_{T,P}$ from differential osmotic pressure measurements may be based on the fundamental differential

 ©1979 The American Physical Society

$$dg = -s\,dT + v\,dP + \Delta\,dx \quad , \tag{1}$$

where $g = x\mu_3 + (1-x)\mu_4 = \mu_4 + x\Delta$ is the Gibbs free energy per mole, s is the entropy per mole, and v is the molar volume.[7] We seek the derivative $(\partial P/\partial x)_{T,\mu_4}$, which may be evaluated as follows:

$$\left(\frac{\partial P}{\partial x}\right)_{T,\mu_4} = -\frac{(\partial\mu_4/\partial x)_{T,P}}{(\partial\mu_4/\partial P)_{T,x}}$$

$$= -\frac{(\partial g/\partial x)_{T,P} - \Delta - x(\partial\Delta/\partial x)_{T,P}}{(\partial g/\partial P)_{T,x} - x(\partial\Delta/\partial P)_{T,x}}$$

$$= \frac{x(\partial\Delta/\partial x)_{T,P}}{v - x(\partial v/\partial x)_{T,P}} = \frac{x}{v_4}\left(\frac{\partial\Delta}{\partial x}\right)_{T,P} , \tag{2}$$

where v_4 is the partial molar volume.

The experiment involves an isothermal cell with two chambers connected by a superleak as shown schematically in Fig. 2. When the superleak is functioning so as to permit osmotic equilibrium involving uniform μ_4 to be established between the chambers at uniform T, a difference $\Delta x = x_l - x_u$ in ^{3}He mole fraction between the chambers will be accompanied by a pressure difference $\Delta P = P_l - P_u$ which will be approximated by the relationship

$$\Delta P \cong (\partial P/\partial x)_{T,\mu_4}\Delta x \quad . \tag{3}$$

Hence, by measuring ΔP in relation to Δx we may determine $(\partial x/\partial\Delta)_{T,P}$ through the relationship

$$\left(\frac{\partial x}{\partial\Delta}\right)_{T,P} = \frac{x}{v_4}\left(\frac{\partial P}{\partial x}\right)^{-1}_{T,\mu_4} \cong \frac{x}{v_4}\left(\frac{\Delta P}{\Delta x}\right)^{-1} \quad . \tag{4}$$

II. EXPERIMENTAL APPARATUS

The experimental cell, shown to scale in Fig. 3, was located at the lower end of a cryostat of conventional design with pumped ^{4}He and ^{3}He stages. The interior of the cell body, which was made primarily of

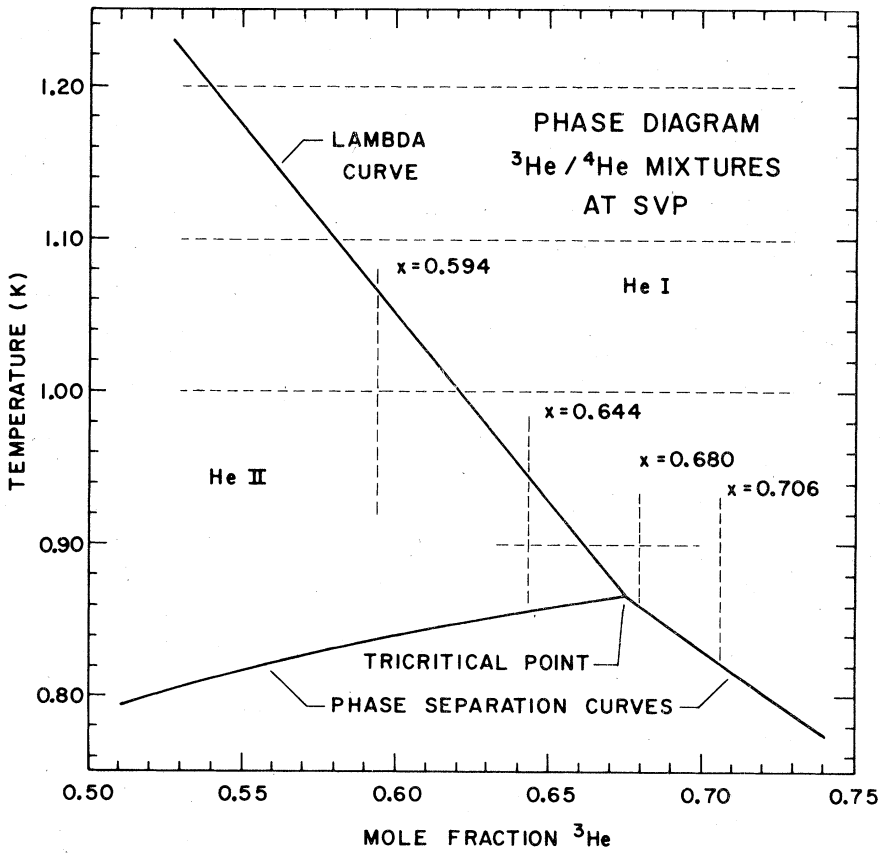

FIG. 1. Phase diagram of ^{3}He/^{4}He mixtures at saturated vapor pressure near the tricritical point. The vertical dashed lines show the regions in which osmotic pressure data were recorded. The horizontal dashed lines show the regions involved in the scaling plot for $(-\partial s/\partial T)_{P,x}$ of Fig. 11.

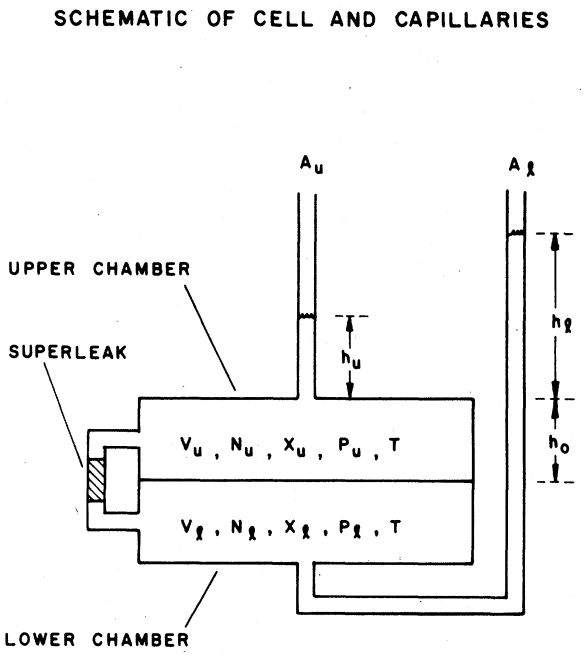

FIG. 2. Schematic drawing of the experimental cell and fill capillaries. The symbols are explained in the text as needed.

two pieces of high-purity copper, was divided into two chambers by a taut 25-μm-thick stainless-steel membrane supported by a stainless-steel ring to which it was welded. An electrically insulated back plate, separated from the membrane by a 6-μm-thick Mylar film, was pressed against it to form a capacitive differential-pressure transducer. The open spaces within the chambers, the main parts of which each had heights of $\sim$2 mm, were filled with OFHC copper felt[22] compressed to $\sim$50% open volume to improve thermal homogeneity within each chamber. The open volume of each chamber was $\sim$1.0 cm^3.

The two chambers of the cell were connected by a superleak located outside the cell at about the same height as the chambers. It consisted of a 15–20 mm length of 1.0-mm-diameter porous Vycor rod,[23] sealed into a high-purity copper bushing with epoxy glue.[24,25] At room temperature, with helium gas at a pressure of 1.0×10^5 Pa on one side and vacuum on the other, the flow rate through the superleak was $\sim 3 \times 10^{-11}$ mole/sec.

Essential to the performance of the experiment was the fact that the superleak enabled osmotic equilibrium of the ^{4}He component to be established between the chambers not only in the superfluid region of the phase diagram for the bulk liquid but also in a portion of the normal-fluid region near the λ curve for $x \gtrsim 0.55$, the tricritical point, and the ^{3}He-rich branch of the phase-separation curve. We believe that this remarkable conduction of ^{4}He by the superleak is due to the phenomenon of wall-film superfluidity.[26,27] At the same time, the superleak prevented any appreciable flow of ^{3}He from taking place, except possibly under some puzzling circumstances mentioned in Sec. III.

Each chamber had a separate fill capillary which led to its own valve at the flange at 4.2 K located at the

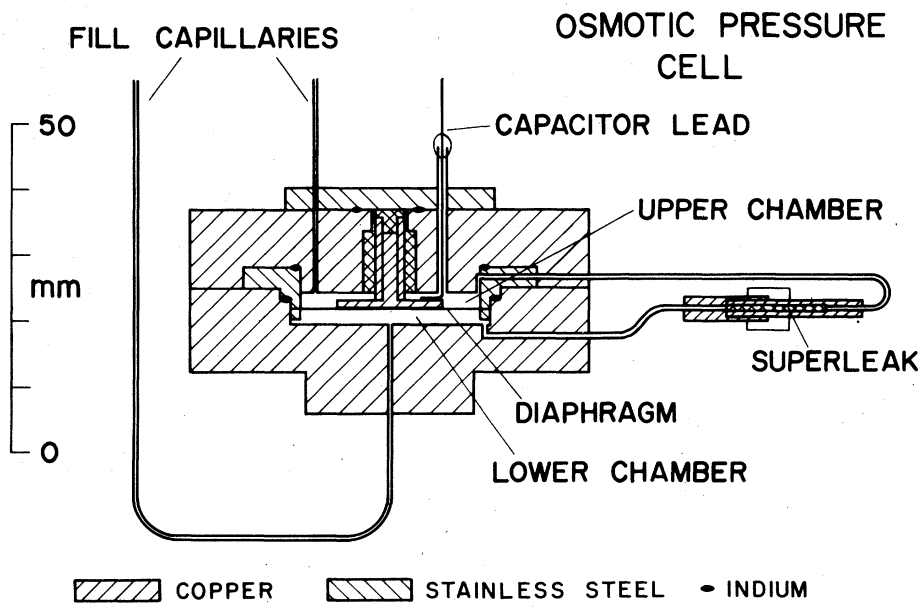

FIG. 3. Scale drawing of the experimental cell.

top of the vacuum can in which the pumped ^{4}He and ^{3}He stages and the cell were located. During an experiment the chambers were filled so that the surfaces of the liquid stood above the cell in these capillaries as depicted in Fig. 2. Osmotic pressure differences between the chambers were accompanied by level differences between capillaries. In order to maintain the liquid in these capillaries at the temperature of the cell, stainless-steel "standpipe" capillaries were soldered to a high-purity copper post 4.8 mm in diameter which extended a distance of 220 mm up from the cell, on which it was mounted, through open wells in the ^{3}He and ^{4}He pots. These capillaries had internal diameters of 0.15 mm, chosen to be as small as possible and yet able to accommodate the thermal expansion of the liquid in the chambers.

The connections between the tops of the standpipes and the valves appeared to be the source of serious instabilities and oscillations in the osmotic pressure difference. Although no single arrangement was entirely satisfactory, the following arrangement was used successfully during much of the work. Short lengths of 0.10-mm-internal-diameter cupronickel tubing partially filled with 0.08-mm-diameter stainless-steel wire connected the standpipes to the valves. Roughly midway along their lengths these capillaries were thermally linked to the ^{4}He pot. This arrangement appeared to be free from the variations mentioned above as long as the temperature of the ^{4}He pot remained above the cell temperature.

The differential pressure transducer formed the capacitive part of the tank circuit of a low-temperature rf oscillator using a G.E. BD-4 back diode.[28,29] The oscillator frequency was ~13 MHz, and its long-term stability was a few parts in 10^7. The signal from the oscillator was amplified at room temperature and fed directly to a frequency counter,[30] with associated digital-to-analog converter[31] and a chart recorder[32] for monitoring the stability and the approach to equilibrium of the osmotic pressure.

The differential-pressure transducer was initially calibrated at low temperature with the superleak removed. After the variation of the empty-cell frequency with temperature was measured, the lower chamber was partially filled with ^{4}He, and the calibration was carried out using the known relationship between the vapor pressure of ^{4}He and temperature.[33] The relationship between frequency and pressure was found to be quite linear up to at least 4 kPa, well above the largest osmotic pressure differences measured. The sensitivity of the pressure measuring system was ~200 Hz/Pa. This sensitivity was checked from time to time with the superleak in place by partially filling the lower chamber with a ^{3}He/^{4}He mixture well above the superfluid onset temperature while the upper chamber remained empty. Here we used the vapor pressure data of Sydoriak and Roberts[34] in connection with the T 62 ^{3}He scale of temperature.[35]

The pumped ^{4}He pot was normally operated at its minimum temperature of ~1.1 K and the ^{3}He pot at its minimum of ~0.5 K. The cell was thermally connected to the ^{3}He pot with a weak link so that it could be regulated at operating temperatures near 1 K with a power of ~5 μW applied to an electrical heater on the cell. The cell was equipped with two germanium resistance thermometers. One, a Cryocal Model CR-500,[36] was used in a conventional three-wire ac bridge circuit with feedback to the cell heater to regulate the cell temperature to within a range of a few μK over periods up to 1 h. The other, an Andonian Cryogenics CG-1,[37] was used in a highly stable and sensitive ac bridge circuit employing a ratio transformer and a low-temperature reference resistor[38] to measure the relative cell temperature to within several μK.[39] The resistance thermometers were calibrated between 0.6 and 1.6 K against the T 62 ^{3}He scale of temperature[35] to ~ ±1 mK using a ^{3}He vapor pressure bulb partially filled with copper felt located directly on the experimental cell.

III. EXPERIMENTAL PROCEDURES AND RESULTS

^{3}He/^{4}He mixtures were prepared at four different values of the ^{3}He mole fraction x near the tricritical value x_t by mixing pure ^{3}He and ^{4}He gases at room temperature. In order to allow for possible fractionation of the samples during the initial condensation into the cell or in subsequent adjustments of the chamber fillings, the mole fractions of the condensed samples were determined by reference to the observed λ or phase-separation temperatures. For this work it was assumed that the tricritical values of T and x are $T_t = 0.867$ K and $x_t = 0.675$,[9,13] that the equation of the λ curve near the tricritical point is

$$x_\lambda(T) = x_t - (0.4082\ \mathrm{K}^{-1})(T - T_t)\ , \tag{5}$$

and that the equation of the ^{3}He-rich branch of the phase-separation curve near the tricritical point is

$$x_{\sigma+}(T) = x_t - (0.6633\ \mathrm{K}^{-1})(T - T_t) + (0.4120\ \mathrm{K}^{-2})(T - T_t)^2\ . \tag{6}$$

These equations were derived from the work of Alvesalo, Berglund, Islander, Pickett, and Zimmermann[7] with adjustments close to the tricritical point as suggested by the analysis of gravitational effects by Watts and Webb.[13] The values of the λ or phase-separation temperatures for our samples together with the resulting mole fractions are listed in Table I.

For each of the four runs at low temperature with a given average mole fraction, several series of data were recorded for several values of the difference $\Delta x = x_l - x_u$ between the mole fraction x_l in the lower chamber and x_u in the upper. These values of Δx

TABLE I. Parameters of the four mixtures studied.

T_λ (K)	T_σ (K)	x
1.067	...	0.594
0.944	(0.856–0.859)[a]	0.644
...	0.860(0.863)[b]	0.680(0.678)[b]
...	0.821(0.824)[b]	0.706(0.704)[b]

[a]Range of uncertainty.

[b]The two values listed represent a range of uncertainty. However, the first number is the most likely value of the quantity tabulated.

were comparable to or less than 10^{-3} in magnitude and of both signs, and were achieved and changed by withdrawing small amounts of sample from one chamber and adding compensating amounts to the other. We could not determine in any direct way the small values of Δx that were used, and consequently we were obliged to normalize our results for $(\partial x/\partial\Delta)_{T,P}$ to external data in a manner to be described in Sec. IV. Once the normalization was established it was possible to estimate the values of Δx for which the data had been recorded.

We were careful during the filling of the cell and the adjustments of Δx to ensure that the liquid surfaces would remain in the standpipe throughout the measurements as thermal expansion and contraction of the sample occurred. The two chambers were filled one at a time above the superleak onset temperature, and the differential-pressure transducer was used to estimate the positions of the liquid surfaces in the standpipes at each step.

Frequency readings from the differential-pressure transducer were recorded at discrete temperature intervals, with intervals of 50 μK being used near T_λ. The use of smaller intervals revealed no further detail. The time required to reach equilibrium after a temperature change ranged from 10 or 15 min to 1 or 2 h, depending on the magnitude of Δx, the size of the temperature change, and on the location of the sample in the phase diagram. The equilibration time became particularly long near the onset temperature of the superleak.

Data recorded over periods of several days both warming and cooling were quite consistent and reproducible, with the exception of long-term drift which occurred in the runs with $x=0.644$, 0.680, and $x=0.706$ during a single prolonged operation of the apparatus at low temperature. At $x=0.644$ this drift was seen only in the normal-fluid region. Although we do not understand the source of this drift, our observations when drift was present were consistent with a model assuming that $|\Delta x|$ decreased at a time rate proportional to $|\Delta P|$. Our frequency data were corrected for drift in accord with this model. The drift occurring in a 12-h period corresponded to a change in Δx of as much as 10%.

When several series of data for different values of Δx at a given average value of $x < x_t$ were compared, it was noted that the temperatures of the extrema in frequency at the λ point sometimes differed. We believe that this effect was due at least in part to slight changes in the average value of x which occurred when Δx was changed. In order to correct for this effect, the temperature scales of some of the series were adjusted to make the extrema coincide. This procedure was not entirely justified, since nonzero Δx and gravitational rounding effects could also have contributed to such temperature shifts. However, the maximum shift applied to any of the series from which the concentration susceptibilities presented here were derived was 70 μK, a rather small amount in comparison to our resolution.

An example of our frequency-versus-temperature data for one value of x, corrected for drift and temperature, is shown in Fig. 4. Here the bulk of the data recorded for $x=0.644$ for five different values of Δx is presented. One value of Δx is very near zero. Then there are two series with small Δx values of both signs and two series with large Δx values of both signs. The cusped features correspond to the λ transition. In this figure the relative frequency at a given temperature is the observed frequency minus the empty-cell frequency at the same temperature minus an arbitrary constant chosen to yield a convenient range of values. It must be kept in mind that because the sample in the upper chamber constituted the dielectric of the capacitor, the empty-cell frequency does not provide a suitable zero-pressure reference level and that there undoubtedly remains some additional extraneous temperature dependence common to all of the series in Fig. 4. We shall discuss our correction for this effect in Sec. IV.

The limits of our resolution are illustrated in Fig. 5 where, for each of the two values of $x < x_t$ studied, the details of a series with a small value of Δx are shown near the λ transition. The λ anomaly for $x=0.594$ is considerably sharper than that for $x=0.644$, even though the Δx values are almost the same. However, as we shall discuss in Sec. V, gravitational broadening effects should have been larger for $x=0.644$ than for $x=0.594$.

IV. DETERMINATION OF $(\partial x/\partial\Delta)_{T,P}$

In calculating the concentration susceptibility $(\partial x/\partial\Delta)_{T,P}$ from the observed osmotic pressure

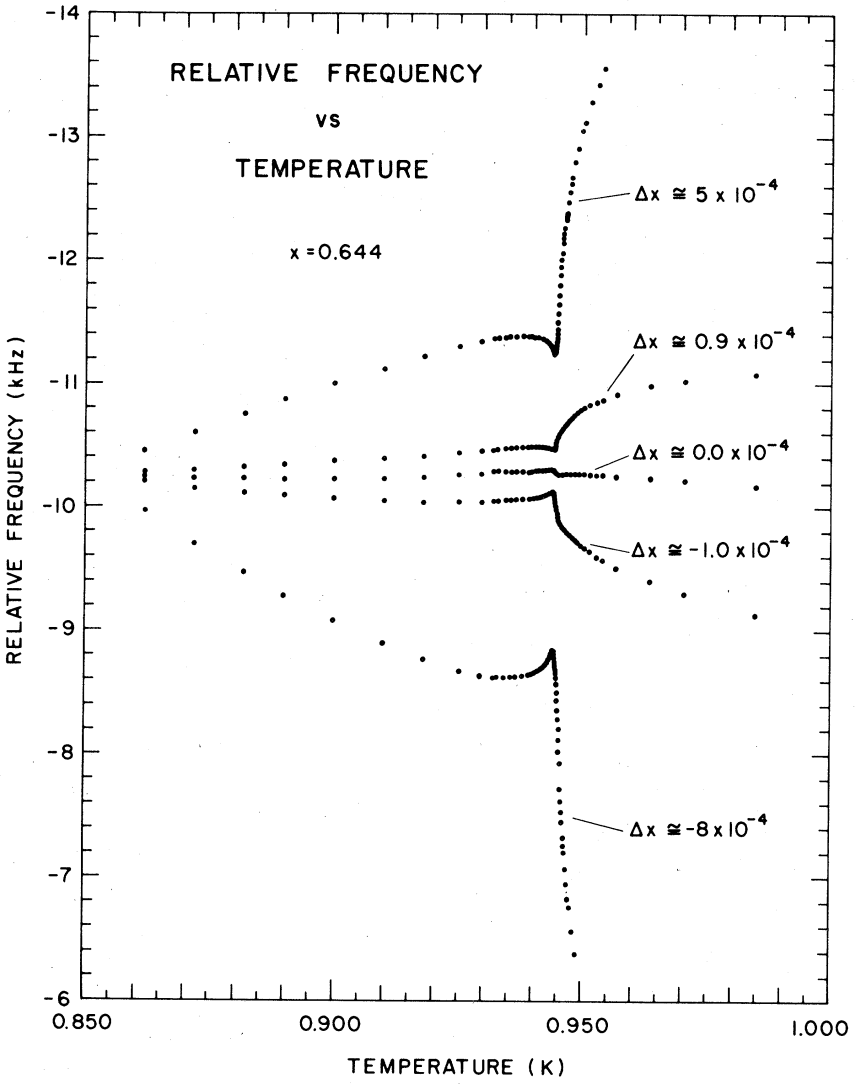

FIG. 4. Relative-frequency-vs-temperature data at $x = 0.644$. Series are shown for five different values of the difference Δx in mole fraction of ^{3}He between lower and upper chambers.

differences, several aspects of the experiment must be considered.

First, as changes in osmotic pressure took place, liquid-level changes in the capillaries occurred which required some flow of ^{4}He through the superleak. Such flow acted to change Δx, and hence Δx was dependent on T through a dependence on ΔP.

Second, changes in the molar volume of the sample with temperature caused changes in the liquid levels in the capillaries. Because of small differences in the chamber volumes, such changes, if unaccompanied by flow of ^{4}He between the chambers, would have tended to alter the level difference from the one corresponding to the correct ΔP. Hence some additional flow of ^{4}He through the superleak was required, and Δx was thus additionally dependent on T through a dependence on molar volume.

Third, because of dielectric-constant effects, the zero-pressure frequency $f_0(T)$ was not well known for any given series. Further, because of small shifts in the value of x in the upper chamber from series to series within a given run and because of possible mechanical disturbances associated with adjusting Δx at the beginning of a new series, $f_0(T)$ may have differed by constant amounts from series to series.

Fourth, gravity caused to exist in each chamber a vertical concentration gradient, which changed with T as $(\partial x/\partial \Delta)_{T,P}$ changed. Because the significant Δx

was that which existed between the bottom of the upper chamber and the top of the lower, i.e., right at the diaphragm, this effect gave another source of variation of Δx with T.

Fifth, there were the averaging effects associated with working with noninfinitesimal Δx.

The remainder of this section describes the difference method of analysis by which $(\partial x/\partial\Delta)_{T,P}$ was obtained from the osmotic pressure measurements. This method corrected for the first three effects. The residual influence of the last two effects is discussed in Sec. V.

The analysis of the first two effects was based on the model shown by the schematic drawing of Fig. 2. By using this model together with Eq. (4) it may be shown that the first effect yields the relationship[21]

$$\Delta P = B(T)\Delta x_0 = \frac{\dfrac{x}{v_4}\left(\dfrac{\partial x}{\partial\Delta}\right)^{-1}_{T,P}}{1+\dfrac{vx^2A}{\rho g v_4^2 V}\left(\dfrac{\partial x}{\partial\Delta}\right)^{-1}_{T,P}}\Delta x_0 \ . \quad (7)$$

Here ΔP equals $P_l - P_u$ and Δx_0 equals $(x_l - x_u)_0$, the difference in x which would exist in the absence of a level difference in the capillaries (i.e., the difference in x that would exist were we by means of pistons in the capillaries to force the levels to be equal). In addition, A is the average cross-sectional area of the capillaries, ρ is the average mass density of the sample, g is the acceleration of gravity, V is the average volume of a chamber, and the remaining thermodynamic quantities are averages over the sample. Equation (7) reduces to Eq. (4) in the limits that $A \to 0$ or $V \to \infty$, in which cases the first effect disappears.

Next, it can be shown that when the second effect is considered assuming zero-level difference between capillaries as thermal expansion takes place, we have[21]

$$\frac{dx_{u0}}{dT} \cong \tfrac{1}{2}x\frac{A_l V_u - A_u V_l}{AV_u}\frac{1}{v_4}\left(\frac{\partial v}{\partial T}\right)_{P,x} , \quad (8a)$$

$$\frac{dx_{l0}}{dT} \cong -\tfrac{1}{2}x\frac{A_l V_u - A_u V_l}{AV_u}\frac{1}{v_4}\left(\frac{\partial v}{\partial T}\right)_{P,x} , \quad (8b)$$

where A_u and A_l are the cross-sectional areas of the upper and lower capillaries, respectively, V_u and V_l are the volumes of the upper and lower chambers, respectively, and the remaining quantities are averages as above. Hence we see that the x_0 values introduced in discussing the first effect acquire a T dependence from the second effect.

Now consider two series of data with different

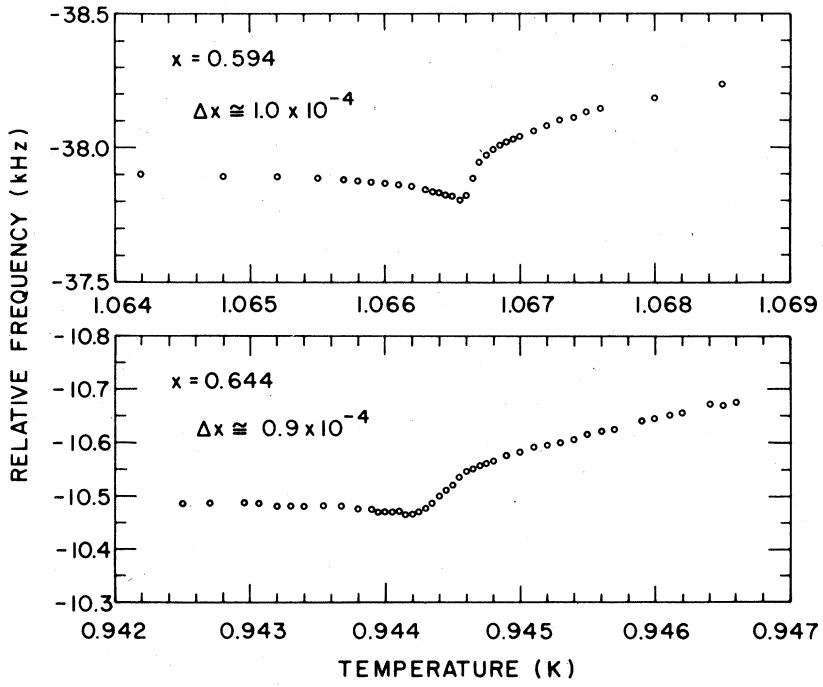

FIG. 5. Details of relative-frequency-vs-temperature data near the λ transition at $x = 0.594$ and $x = 0.644$. In each case, data from a series with a small value of $\Delta x > 0$ are shown.

values of Δx for the same average value of x. We may write

$$f_i(T) - f_0(T) - \delta f_i = K \Delta P_i(T) = KB(T) \Delta x_{0i}(T) \quad , \tag{9a}$$

$$f_j(T) - f_0(T) - \delta f_j = K \Delta P_j(T) = KB(T) \Delta x_{0j}(T) \quad , \tag{9b}$$

where the two series are denoted i and j. Here we have written the zero-pressure frequency for each series as $f_0(T) + \delta f$ to reflect a possible constant series-dependent shift δf from a reference-temperature dependence $f_0(T)$ common to all of the series in a given run. However, since in the end there was little consistent evidence for variations in δf from series to series and the δf quantities were allowed to have very little influence on the results,[21] we will not consider them further here. The quantity K is the sensitivity of the differential-pressure transducer.

Subtracting Eq. (9a) from Eq. (9b) we have

$$f_j(T) - f_i(T) = KB(T)[\Delta x_{0j}(T) - \Delta x_{0i}(T)] = KB(T)\{[x_{l0j}(T) - x_{l0i}(T)] - [x_{u0j}(T) - x_{u0i}(T)]\} \quad . \tag{10}$$

Because the temperature dependences of x_{u0j} and x_{u0i} as given by Eq. (8a) are very nearly the same, as are those of x_{l0j} and x_{l0i} as given by Eq. (8b), the quantities in brackets in Eq. (10) will be very nearly temperature independent, and $B(T)$ will simply be proportional to $f_j(T) - f_i(T)$. Hence by analyzing differences between series we eliminate the need to know $A_l V_u - A_u V_l$ and $f_0(T)$, and the second effect and the most difficult part of the third effect are automatically corrected for. The resulting proportionality between $B(T)$ and $f_j(T) - f_i(T)$ for a given pair of series involves one unknown constant, which can be determined by reference to external data for $(\partial x/\partial \Delta)_{T,P}$ at a single temperature. Then $B(T)$ and from it $(\partial x/\partial \Delta)_{T,P}$ can be calculated from values of $f_j(T) - f_i(T)$ at other temperatures.

Values of $(\partial x/\partial \Delta)_{T,P}$ for each of the four values of x studied were determined by the method described above and are listed in Table II and displayed in Fig. 6. In each case the values are those derived from a single pair of series deemed to represent $(\partial x/\partial \Delta)_{T,P}$ most accurately. For $x = 0.594$ the two series chosen had $\Delta x \cong -0.6 \times 10^{-4}$ and 1.0×10^{-4}; for $x = 0.644$ they had $\Delta x \cong -1.0 \times 10^{-4}$ and 0.9×10^{-4}. For $x = 0.680$ the series chosen had $\Delta x \cong 0.3 \times 10^{-4}$ and 0.8×10^{-4}; for $x = 0.706$ they had $\Delta x \cong \pm 4.0 \times 10^{-4}$. Values for v_4 and v were derived from the work of Kerr.[40]

Our data for $x = 0.594$ were normalized at $T = 0.950$ K and for the other values of x at $T = 0.900$ K to values interpolated from the tabulated results of Goellner, Behringer, and Meyer (GBM)[11] for $(\partial x/\partial \Delta)_{T,P}$ derived from vapor-pressure measure-

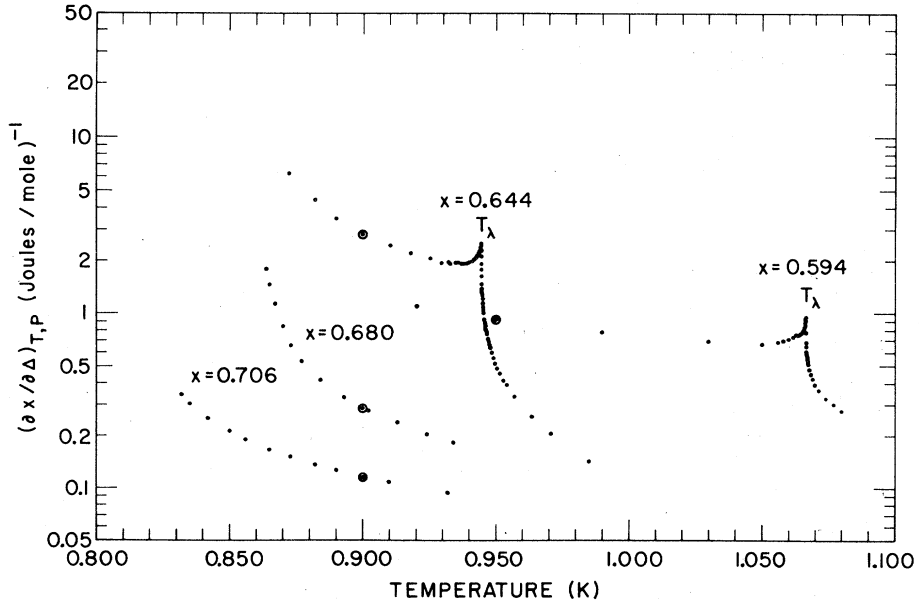

FIG. 6. Concentration susceptibility vs temperature at the four values of x studied. The large circles mark the points at which these results are normalized to those of GBM. (See Ref. 11).

TABLE II. Concentration susceptibility as a function of temperature for four values of mole fraction.

T (K)	$(\partial x/\partial\Delta)_{T,P}$ (J/mole)$^{-1}$	T (K)	$(\partial x/\partial\Delta)_{T,P}$ (J/mole)$^{-1}$	T (K)	$(\partial x/\partial\Delta)_{T,P}$ (J/mole)$^{-1}$	T (K)	$(\partial x/\partial\Delta)_{T,P}$ (J/mole)$^{-1}$
$x=0.594$		$x=0.644$		$x=0.644$ (cont'd.)		$x=0.680$	
1.080 100	0.275	0.984 800	0.139	0.944 350	2.073	0.934 000	0.180
1.077 000	0.301	0.970 600	0.203	0.944 300	2.238	0.924 000	0.202
1.074 200	0.327	0.963 600	0.252	0.944 250	2.349	0.913 000	0.234
1.071 300	0.363	0.956 800	0.328	0.944 200	2.428	0.902 000	0.275
1.070 000	0.391	0.954 000	0.384	0.944 150	2.469	0.900 000	0.288
1.069 100	0.422	0.952 800	0.405	0.944 100	2.428	0.893 000	0.331
1.068 500	0.446	0.951 400	0.443	0.944 050	2.428	0.884 000	0.415
1.068 000	0.477	0.950 200	0.478	0.944 000	2.388	0.877 000	0.530
1.067 600	0.499	0.949 600	0.500	0.943 950	2.389	0.873 000	0.652
1.067 500	0.505	0.948 900	0.544	0.943 900	2.350	0.870 000	0.836
1.067 400	0.519	0.948 300	0.584	0.943 800	2.350	0.867 000	1.121
1.067 300	0.529	0.947 700	0.627	0.943 680	2.275	0.865 000	1.434
1.067 200	0.541	0.947 500	0.647	0.943 540	2.240	0.864 000	1.788
1.067 100	0.561	0.947 200	0.669	0.943 400	2.205		
1.067 000	0.578	0.946 900	0.703	0.943 300	2.171		
1.066 950	0.585	0.946 600	0.739	0.943 200	2.171	$x=0.706$	
1.066 900	0.592	0.946 500	0.745	0.943 060	2.105		
1.066 850	0.603	0.946 400	0.752	0.942 950	2.105	0.932 000	0.092
1.066 800	0.615	0.946 200	0.778	0.942 700	2.105	0.910 000	0.105
1.066 750	0.646	0.946 100	0.791	0.942 500	2.074	0.900 000	0.114
1.066 700	0.685	0.946 000	0.805	0.942 200	2.043	0.890 000	0.124
1.066 650	0.778	0.945 900	0.819	0.942 000	2.013	0.882 000	0.133
1.066 600	0.913	0.945 700	0.856	0.941 700	1.984	0.873 000	0.148
1.066 550	0.964	0.945 600	0.880	0.941 500	1.984	0.865 000	0.164
1.066 500	0.941	0.945 500	0.896	0.940 800	1.928	0.856 000	0.188
1.066 450	0.927	0.945 400	0.930	0.940 200	1.928	0.850 000	0.210
1.066 400	0.920	0.945 300	0.956	0.939 600	1.901	0.842 000	0.248
1.066 350	0.906	0.945 200	0.983	0.939 000	1.875	0.835 000	0.300
1.066 300	0.893	0.945 100	1.022	0.937 800	1.875	0.832 000	0.339
1.066 200	0.866	0.945 000	1.073	0.936 600	1.875		
1.066 100	0.854	0.944 900	1.117	0.935 500	1.901		
1.066 000	0.848	0.944 800	1.188	0.934 300	1.901		
1.065 900	0.835	0.944 750	1.227	0.932 800	1.875		
1.065 800	0.823	0.944 700	1.267	0.932 000	1.928		
1.065 700	0.812	0.944 650	1.310	0.929 600	1.901		
1.065 500	0.800	0.944 600	1.354	0.925 200	2.013		
1.065 200	0.784	0.944 550	1.451	0.918 000	2.171		
1.064 800	0.773	0.944 500	1.599	0.910 000	2.389		
1.064 200	0.762	0.944 450	1.750	0.900 000	2.800		
1.063 500	0.747	0.944 400	1.874	0.890 000	3.430		
1.062 800	0.747			0.882 000	4.376		
1.061 400	0.727			0.872 000	6.173		
1.060 000	0.712						
1.058 000	0.698						
1.056 000	0.685						
1.050 000	0.667						
1.030 000	0.694						
0.990 000	0.784						
0.950 000	0.920						
0.920 000	1.098						

ments. The normalizations are somewhat arbitrary in view of some differences in temperature dependences between our data and theirs even well away from the λ transition. A comparison of our results for $(\partial x/\partial\Delta)_{T,P}$ at $x=0.644$ with an interpolation of those of Ryschkewitsch, Doiron, Chan, and Meyer[15] derived from gravitational concentration-gradient measurements shows that at $T=0.934$ K their value is 25% smaller.

It should be kept in mind that because of the nonlinear relation between $(\partial x/\partial\Delta)_{T,P}$ and $B(T)$ an alteration in the normalization of our data involves more than simple multiplication by a constant. In the denominator of $B(T)$ in Eq. (7) the coefficient of $(\partial x/\partial\Delta)_{P,T}^{-1}$ ranged from 0.25 to 0.43 (J/mole)$^{-1}$. As a result the denominator itself, whose departure from unity measures the amount of correction due to the first effect, ranged from 1.06 for large values of $(\partial x/\partial\Delta)_{T,P}$ to 5.7 for small values. As can be seen from Eq. (7), a denominator $\gg 1$ represents a situation in which ΔP is relatively insensitive to $(\partial x/\partial\Delta)_{T,P}$. The denominator remained $\lesssim 2$ for all of the data subject to critical analysis near T_λ.

V. EFFECTS OF GRAVITY AND OF NONINFINITESIMAL Δx

In the earth's gravitational field we may write the gravitational-chemical potentials of the ^{3}He and ^{4}He constituents per mole at height y

$$\mu_{3g}=\mu_3(T,P,x)+m_3gy \quad , \tag{11a}$$

$$\mu_{4g}=\mu_4(T,P,x)+m_4gy \quad , \tag{11b}$$

where μ_3 and μ_4 are the ordinary chemical potentials and m_3 and m_4 are the masses per mole of ^{3}He and ^{4}He, respectively. In equilibrium, μ_{3g} and μ_{4g} must be uniform. We may also write

$$\Delta_g=\mu_{3g}-\mu_{4g}=\Delta(T,P,x)+(m_3-m_4)gy \quad . \tag{12}$$

Since Δ_g must also be uniform in equilibrium, we have

$$\left[\frac{d\Delta_g}{dy}\right]_T=\left(\frac{\partial\Delta}{\partial P}\right)_{T,x}\left[\frac{dP}{dy}\right]_T+\left(\frac{\partial\Delta}{\partial x}\right)_{T,P}\left[\frac{dx}{dy}\right]_T + (m_3-m_4)g=0 \quad . \tag{13}$$

Solving for $[dx/dy]_T$, employing the Maxwell relation $(\partial\Delta/\partial P)_{T,x}=(\partial v/\partial x)_{T,P}$ that follows from Eq. (1), and recognizing that $[dP/dy]_T=-\rho g$, we have

$$\left[\frac{dx}{dy}\right]_T=\left(\frac{\partial x}{\partial\Delta}\right)_{T,P}\left[(m_4-m_3)+\rho\left(\frac{\partial v}{\partial x}\right)_{T,P}\right]g \tag{14}$$

for the gravitational gradient in x within each chamber. By chance, the magnitudes of the two terms in the brackets on the right are nearly equal in the region of interest to us.

In osmotic equilibrium, μ_{4g} is uniform throughout the system. If we use the subscript u to denote an arbitrary location in the upper chamber and l to denote such a location in the lower, then we have

$$\mu_4(T,P_u,x_u)+m_4gy_u=\mu_4(T,P_l,x_l)+m_4gy_l \quad . \tag{15}$$

Using Eq. (2) and the relationship $v_4=(\partial\mu_4/\partial P)_{T,x}$, we may expand Eq. (15) to first order in the differences between upper and lower chambers to obtain the equation

$$P_l-P_u\cong\frac{x}{v_4}\left(\frac{\partial x}{\partial\Delta}\right)_{T,P}^{-1}(x_l-x_u)-\frac{m_4g}{v_4}(y_l-y_u) \quad . \tag{16}$$

Since we measure the pressure difference between the top of the lower chamber and the bottom of the upper, for which the y values are the same, we have the relationship

$$\Delta P=P_{lt}-P_{ub}\cong\frac{x}{v_4}\left(\frac{\partial x}{\partial\Delta}\right)_{T,P}^{-1}(x_{lt}-x_{ub}) \quad . \tag{17}$$

where now the additional subscripts t and b denote top and bottom, respectively.

The temperature dependence of $\Delta x=x_{lt}-x_{ub}$ near the λ transition is depicted schematically in Fig. 7 for the case in which we have $\Delta\bar{x}=\bar{x}_l-\bar{x}_u>0$. Here the bars denote averages. We see that Δx will vary with T in a complicated manner. If $\Delta\bar{x}<0$, Δx varies with T in a different manner and may even differ in sign from $\Delta\bar{x}$ if $\Delta\bar{x}$ is small. However, note that if the λ curve had zero slope, the difference method of analysis would automatically correct for such variations in Δx, insofar as variations of $(\partial x/\partial\Delta)_{T,P}$ parallel to the λ curve could be ignored. Note that the effects of noninfinitesimal $\Delta\bar{x}$ are being taken into account here as well as those of gravity.

Thus the effects of gravity as well as those of working with noninfinitesimal values of $\Delta\bar{x}$ come into our results mainly because of the nonzero slope of the λ curve. Their foremost influence will be to introduce an effective irresolution in temperature which is most significant near the λ curve and whose magnitude there may be estimated roughly to be less than or approximately equal

$$\Delta T=|dT_\lambda/dx|(|\Delta\bar{x}|+x_{it}-x_{ib}) \quad ,$$

where $x_{it}-x_{ib}$ is the difference in x between the top and bottom of a single chamber.

For $\Delta\bar{x}=1.0\times10^{-4}$ by itself, we would have $\Delta T=2.4\times10^{-4}$ K. For a uniform $(\partial x/\partial\Delta)_{T,P}=1.0$ (J/mole)$^{-1}$, approximately the maximum value measured at $x=0.594$, $x_{it}-x_{ib}$ in a chamber 2 mm high would be $\approx0.4\times10^{-4}$, and ΔT from this source alone would be $\approx1.0\times10^{-4}$ K. For a uniform $(\partial x/\partial\Delta)_{T,P}=2.5$ (J/mole)$^{-1}$, approximately the maximum value

measured at $x=0.644$, $x_{it}-x_{ib}$ would be $\approx 1.0\times10^{-4}$ and ΔT would be $\approx 2.4\times10^{-4}$ K. Hence the rounding due to gravity near the λ curve in our cell appears to have been comparable to that due to the noninfinitesimal values of $\Delta\bar{x}$ that we used for determining $(\partial x/\partial\Delta)_{T,P}$. The greater sharpness of the λ anomaly for $x=0.594$ than for $x=0.644$ shown in Fig. 5 may reflect the smaller gravitational rounding expected for the smaller value of x.

Further comments on these effects will be found in Sec. VI.

VI. CRITICAL BEHAVIOR AT THE λ CURVE

Our results for $(\partial x/\partial\Delta)_{T,P}$ show a pronounced peak at the λ curve, a feature which was not observed in the work of GBM[11] at these values of x nor in that of Watts and Webb[13] but which has been observed in the recent work of Ryschkewitsch, Doiron, Chan, and Meyer (RDCM).[15,16] Plots of $(\partial x/\partial\Delta)_{T,P}$ at constant x vs $\ln|t|$, where t equals $[T-T_\lambda(x)]/T_\lambda(x)$, near the λ curve are shown in Fig. 8. Somewhat arbitrarily, but with the guidance of the fitting results discussed below, we chose T_λ to be 1.066 550 K for $x=0.594$, the temperature of the maximum observed value of $(\partial x/\partial\Delta)_{T,P}$. For $x=0.644$, T_λ was chosen to be 0.944 350 K, 200 μK greater than the temperature of the maximum.

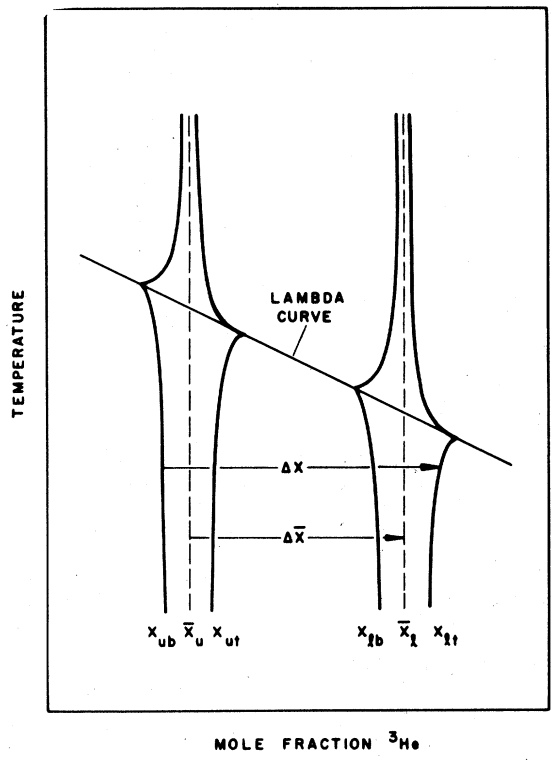

FIG. 7. Schematic diagram of the influence of gravity near the λ curve on the values of x at the tops and bottoms of the upper and lower chambers.

For $x=0.594$, the data points for $2\times10^{-4}\lesssim|t|$ lie in reasonably straight lines consistent with $(\partial x/\partial\Delta)_{T,P}\propto\ln|t|+a$ constant for T both above and below T_λ. The deviation for $|t|\lesssim 2\times10^{-4}$ is consistent with the irresolution estimates of Sec. V. For $x=0.644$, the data points for $3\times10^{-4}\lesssim|t|\lesssim 6\times10^{-3}$ lie nearly in a straight line, but for $T>T_\lambda$ they show a suggestion of upward curvature, which could conceivably be shared with the curve for $T<T_\lambda$ with a small shift in T_λ. The deviation for $|t|\lesssim 3\times10^{-4}$ is consistent with the estimates in Sec. V of a somewhat larger region of gravitational rounding for $x=0.644$ than for $x=0.594$.

In order to examine further the critical behavior of $(\partial x/\partial\Delta)_{T,P}$ near the λ curve, we have fitted to our data at constant x the expression

$$\left(\frac{\partial x}{\partial\Delta}\right)_{T,P}=\frac{A_\pm}{\alpha_\pm}(|t|^{-\alpha_\pm}-1)+B_\pm\ , \tag{18}$$

where $\alpha_\pm$, $A_\pm$, and $B_\pm$ are constants, the upper sign applying for $t>0$ and the lower for $t<0$. This expression reduces to

$$(\partial x/\partial\Delta)_{T,P}=-A_\pm\ln|t|+B_\pm \tag{19}$$

in the limits $\alpha_\pm\to 0$.

Fitting was carried out by using a nonlinear least-squares program to select optimum values for $A_\pm$, $B_\pm$, T_λ and various sets of $\alpha_\pm$. The data fitted were those lying in intermediate regions above and below the λ transition, far enough away to avoid the major irresolution effects discussed in Sec. V but close enough to lie plausibly within the critical region.

Selected fitting results are presented in Table III along with the temperature ranges of the data fitted. The parameter errors quoted are simply the statistical standard deviations of the parameter values derived in the fitting process. It should be remarked that the parameter values are highly correlated, so that a shift in one parameter requires shifts in other parameters to minimize the loss in quality of the fitting. The standard error (SE) in $(\partial x/\partial\Delta)_{T,P}$ equals $[\Sigma/(N-n)]^{1/2}$, where Σ is the sum of the squares of the deviations of the data points from the fitting formula, N is the number of data points, and n is number of free fitting parameters. Note that the normalizations of the data used for these fittings differ somewhat from those used elsewhere in this paper.

For $x=0.594$, two fittings are listed, one with all parameters free and one with the values of $\alpha_\pm$ both fixed essentially at zero. Although the first fitting indicates a slight preference for somewhat-greater-than-zero values for both $\alpha_\pm$, corresponding to a weakly divergent $(\partial x/\partial\Delta)_{T,P}$, the quality of both fittings is good and there is no strong evidence for the

TABLE III. Fitting results for the concentration susceptibility as a function of T at constant x near the λ transition for two values of x. The data were fitted with Eq. (18). SE is the standard error.

T_λ (K)	α_+	α_-	A_+ $(J/mole)^{-1}$	A_- $(J/mole)^{-1}$	B_+ $(J/mole)^{-1}$	B_- $(J/mole)^{-1}$	SE in $(\partial x/\partial\Delta)_{T,P}$ $(J/mole)^{-1}$
			$x=0.594$				
			Normalization: $(\partial x/\partial\Delta)_{T,P}=0.980$ $(J/mole)^{-1}$ at $T=0.950$ K				
1.06650 ±0.00004	0.033 ±0.037	0.052 ±0.057	0.078 ±0.016	0.038 ±0.013	−0.061 ±0.047	0.538 ±0.042	±0.0043
1.06650 ±0.00002	0.001 (fixed)	0.001 (fixed)	0.095 ±0.002	0.054 ±0.001	−0.116 ±0.009	0.485 ±0.008	±0.0047
Data fitted in range $-1.0\times10^{-2}\leq t\leq-1.9\times10^{-4}$ and $1.9\times10^{-4}\leq t\leq1.3\times10^{-2}$ relative to $T_\lambda=1.06655$ K.							
			$x=0.644$				
			Normalization: $(\partial x/\partial\Delta)_{T,P}=2.825$ $(J/mole)^{-1}$ at $T=0.900$ K				
0.94438 ±0.00005	0.089 ±0.043	0.197 ±0.066	0.149 ±0.034	0.058 ±0.023	−0.462 ±0.110	1.369 ±0.110	±0.0108
0.94426 ±0.00005	0.188 ±0.038	0.001 (fixed)	0.089 ±0.018	0.185 ±0.008	−0.262 ±0.072	0.919 ±0.045	±0.0117
0.94447 ±0.00001	0.001 (fixed)	0.27 ±0.06	0.24 ±0.004	0.039 ±0.014	−0.73 ±0.02	1.46 ±0.09	±0.011
0.94446 ±0.00002	0.001 (fixed)	0.001 (fixed)	0.242 ±0.004	0.215 ±0.005	−0.740 ±0.025	0.764 ±0.032	±0.0138
Data fitted in range $-0.6\times10^{-2}\leq t\leq-4.8\times10^{-4}$ and $3.2\times10^{-4}\leq t\leq1.3\times10^{-2}$ relative to $T_\lambda=0.94435$ K.							

values of $\alpha_\pm$ being other than zero or close to it, consistent with the impression given by Fig. 8. For $x=0.644$, four fittings are listed, one with all parameters free, two with one α value or the other fixed essentially at zero, and one with both α values fixed essentially at zero. Here the quality of the last fitting appears to be significantly lower than that of the others, and there appears to be a clear preference for one or both of the α values to be greater than zero, although there appears to be no strong preference among the first three possibilities. This result confirms the suggestion of curvature given by the lowest plot in Fig. 8.

It has occurred to us that the effects of gravity in our cell, when considered in detail, might cause the effective values of α determined above to deviate from the actual values. In particular, we are interested in the possibility that actual zero α values might result in effective values greater than zero at $x=0.644$. We are attempting to investigate this possibility by carrying out model calculations based on the thermodynamics presented in Sec. V together with Eq. (19) ($\alpha_\pm=0$).

Plots similar to Fig. 8 given by RDCM[15] of their data at $x=0.603$ appear rather linear over the range $5\times10^{-5}<|t|<8\times10^{-3}$, a range which includes significantly smaller values of $|t|$ than our range of linearity for $x=0.594$. Rounding effects near the λ transition seem to be playing a smaller role in their experiments than in ours.

VII. TRICRITICAL SCALING

Riedel, Meyer, and Behringer (RMB)[12] proposed a very simple form of tricritical scaling relationship for $(\partial x/\partial\Delta)_{T,P}$ in the T,x plane and showed that within a certain region of the phase diagram near the tricritical point the data of GBM[11] satisfied this relationship. Since the data of GBM did not show the cusp that we and RDCM[15,16] have observed at the λ curve, it is of particular interest to see whether our data obey this relationship in the vicinity of the λ curve.

RMB define a variable z given by the expression

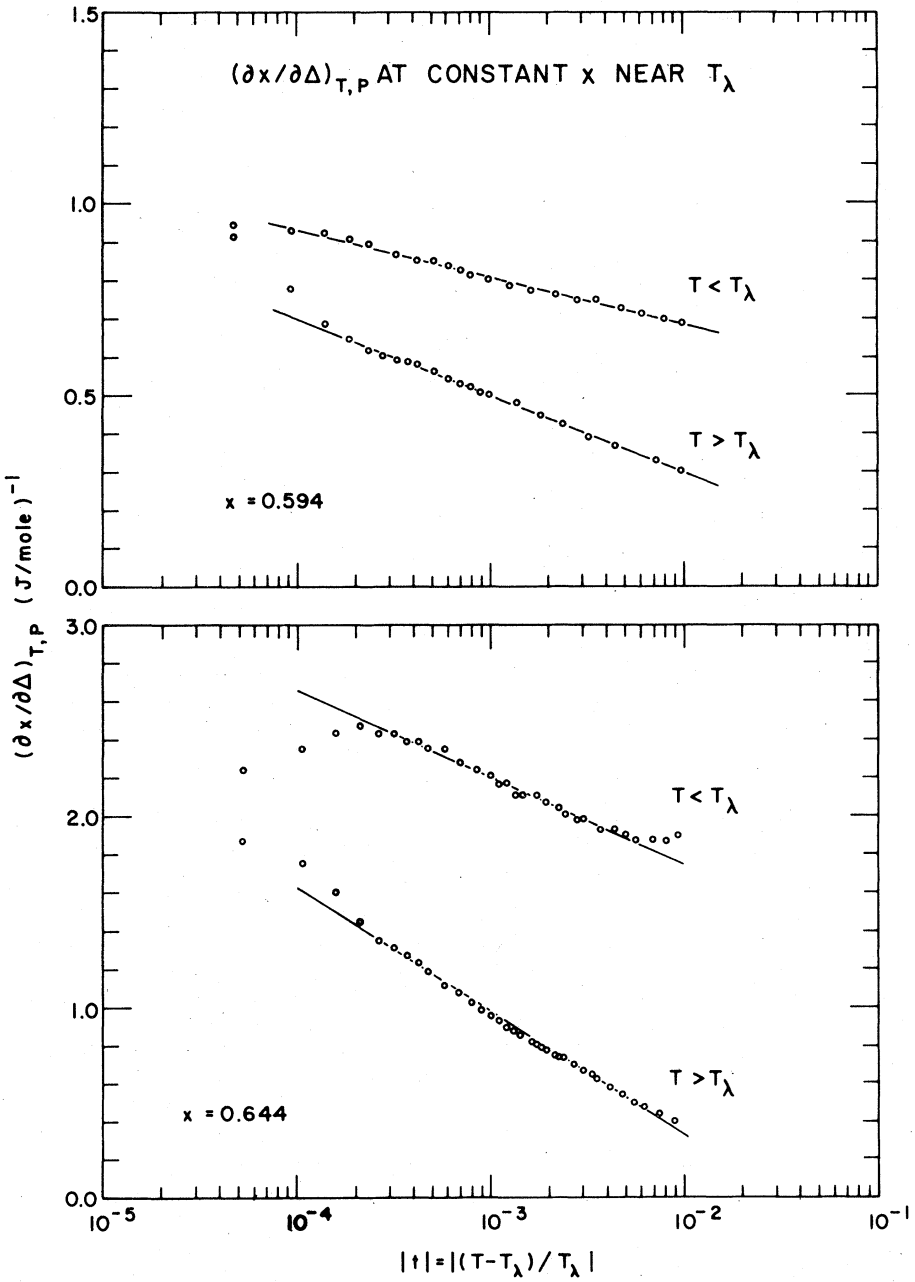

FIG. 8. Semilog plots of the concentration susceptibility versus the absolute value of the reduced temperature near the λ transition along paths of constant x. The lines are simply straight lines drawn to guide the eye.

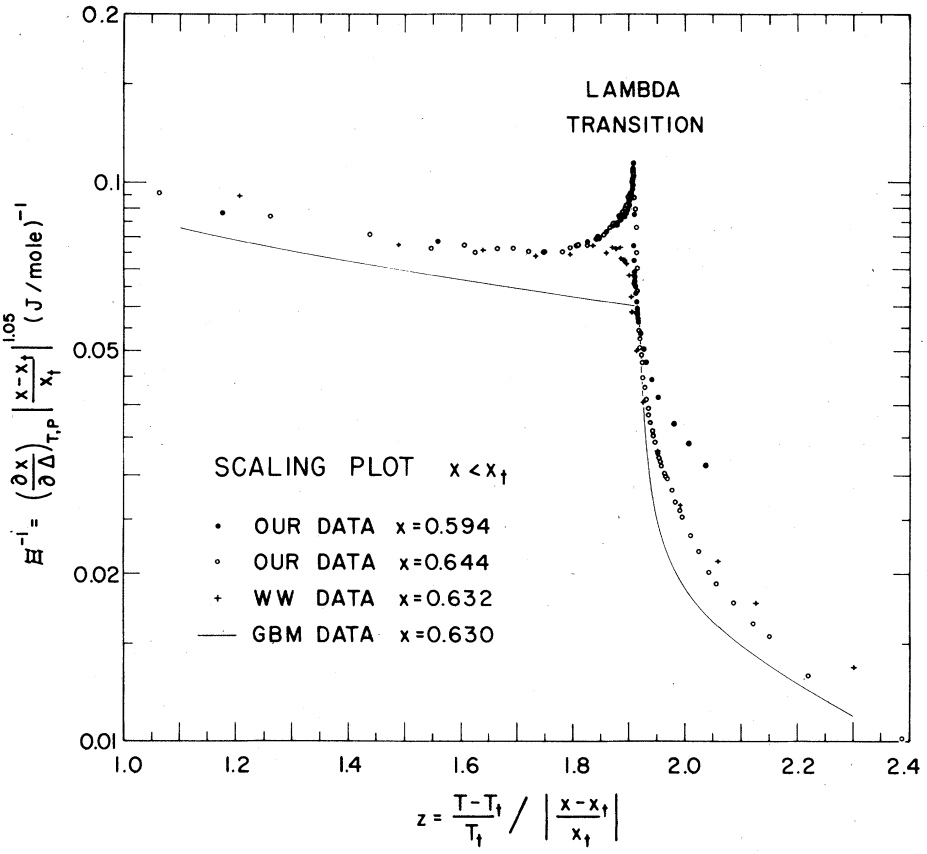

FIG. 9. Plot of our results at $x=0.594$ and $x=0.644$, those of WW at $x=0.632$ (see Ref. 13), and those of GBM at $x=0.630$ (see Refs. 11 and 15), in the scaling form of RMB (see Ref. 12). For our data and those of WW we have assumed $T_t=0.867$ K and $x_t=0.675$. For this plot our data for $(\partial x/\partial\Delta)_{T,P}$ at $x=0.594$ were normalized to 0.950 $(\text{J/mole})^{-1}$ at $T=0.950$ K.

$$z=\frac{\tau}{|\chi|^{1/\omega}}\ , \tag{20}$$

where

$$\tau=(T-T_t)/T_t,\quad \chi=(x-x_t)/x_t\ ,$$

and ω is a constant exponent. Curves of constant z are curves radiating from the tricritical point. In addition, RMB define a reduced inverse concentration susceptibility Ξ given by the expression

$$\Xi=\frac{\left(\dfrac{\partial x}{\partial\Delta}\right)^{-1}_{T,P}}{|\chi|^{\delta-1}}\ , \tag{21}$$

where δ is another constant exponent. Their scaling hypothesis is that Ξ is a function of z alone. In this relationship, the tricritical behavior of $(\partial x/\partial\Delta)_{T,P}$ as a function of χ, as observed in pure form along a curve of constant z, is carried by the exponent $\delta-1$, while the λ critical behavior, as observed along some path of variable z cutting the lambda curve, is carried in the detailed form of $\Xi(z)$. Since the λ curve itself must be a curve of constant z, ω is taken equal to unity, consistent with the remarkable linearity of that curve near the tricritical point. RMB find δ to be 2.05.

In order to test this relationship we have plotted in Fig. 9 the function $\Xi^{-1}=(\partial x/\partial\Delta)_{T,P}|\chi|^{1.05}$ vs z for our data at $x=0.594$ and $x=0.644$ near the λ transition. Also plotted are the results of Watts and Webb (WW)[13] at $x=0.632$ and those of GBM at $x=0.630$ as given by RDCM. We take the latter as representing the RMB scaling form for $x<x_t$. It should be emphasized that since our data require external normalization at each value of x, they provide no evidence regarding the $1/|\chi|^{\delta-1}$ dependence of the scaling function or the value of δ. In fact, for the purpose of enhancing in Fig. 9 the coincidence of our data near the λ transition for the two values of x, the normalization of $(\partial x/\partial\Delta)_{T,P}$ for $x=0.594$ was increased from 0.920 to 0.950 $(\text{J/mole})^{-1}$ at $T=0.950$ K.

It will be seen that in the immediate vicinity of the λ transition at $z_\lambda = 1.907$ and for $z < z_\lambda$ the scaling relationship is well obeyed by our data, even though the form of the relationship at the λ curve is quite different from that of WW or GBM. However, for increasing $z > z_\lambda$ our data for $x = 0.594$ seem to be diverging from those for $x = 0.644$. These observations seem to be inconsistent with the fact that while our data at $x = 0.594$ are just on the edge of the RMB scaling region for $z < z_\lambda$, they lie well within the region for $z > z_\lambda$.

In Fig. 10 we have plotted Ξ^{-1} vs z for our data at $x = 0.680$ and $x = 0.706$. Also plotted in Fig. 10 is the scaling form of RMB for $x > x_t$. There appears to be a reasonable degree of consistency among the three sets of data in this form.

We note that an analogous tricritical scaling relationship for the Ising-like antiferromagnet dysprosium aluminum garnet has been presented by Giordano and Wolf.[41]

It is interesting to recognize that the RMB scaling hypothesis for $(\partial x/\partial \Delta)_{T,P}$ implies the existence of a scaling relationship for $(\partial s/\partial T)_{P,x} = c_{P,x}/T$ as a function of τ and χ.[42] This relationship may be written

$$\left(-\frac{\partial s}{\partial T}\right)_{P,x} = \chi\phi(\tau) + \psi(\tau) + |\tau|^{-\alpha_u} j\left(\frac{\chi}{|\tau|^{\omega}}\right), \qquad (22)$$

where ϕ and ψ are unknown functions of integration and j is a scaling function remotely related to Ξ through a succession of two integrations and differentiations. The exponent $\alpha_u = 2 - \omega(\delta + 1)$ is that which governs the behavior of $c_{P,x}/T$ for $\tau > 0$ at $\chi = 0$.

We may make an experimental test of this relationship without *a priori* knowledge of the forms of ϕ, ψ, or j. From Eq. (22) may be derived the relationship

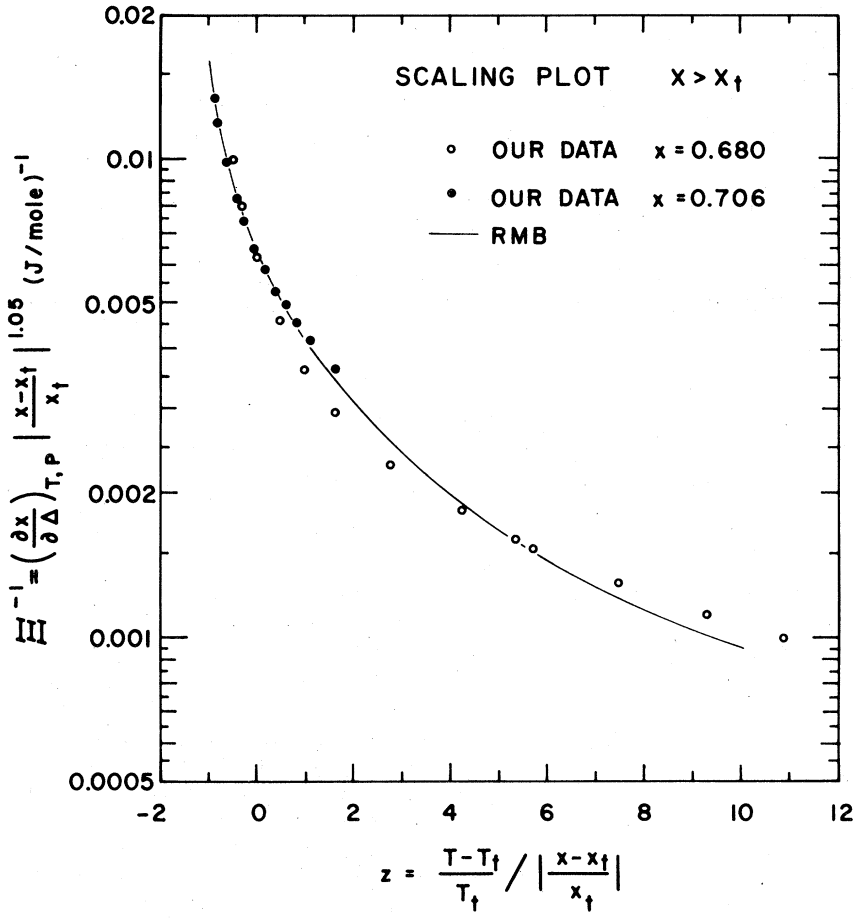

FIG. 10. Plot of our results at $x = 0.680$ and $x = 0.706$ in the scaling form of RMB (see Ref. 12) together with the scaling curve for $x > x_t$ derived by RMB from the data of GBM. (See Ref. 11.)

$$\frac{\left[-\frac{\partial s}{\partial T}\right]_{P,x}(\tau,\chi)-\left[-\frac{\partial s}{\partial T}\right]_{P,x}(\tau,\chi_0)}{\chi-\chi_0}$$

$$=\phi(\tau)+\frac{|\tau|^{-\alpha_u}}{\chi-\chi_0}\left[j\left(\frac{\chi}{|\tau|^{\omega}}\right)-j\left(\frac{\chi_0}{|\tau|^{\omega}}\right)\right], \quad (23)$$

where the arbitrary function $\chi_0(\tau)$ gives a reference value of χ at any given value of τ. Let us choose $\chi_0(\tau)$ to have the form

$$\chi_0(\tau)=a_0|\tau|^{\omega}, \quad (24)$$

where a_0 is a constant, so that $\chi_0(\tau)$ corresponds to a curve of constant $z=z_0$. ($|a_0|=1/|z_0|^{\omega}$). Then Eq. (23) may be written

$$\frac{\left[-\frac{\partial s}{\partial T}\right]_{P,x}(\tau,\chi)-\left[-\frac{\partial s}{\partial T}\right]_{P,x}(\tau,\chi_0)}{(\chi-\chi_0)|\tau|^{-\alpha_u-\omega}}=\xi(\tau)+k\left(\frac{\chi}{|\tau|^{\omega}}\right), \quad (25)$$

where $\xi(\tau)=\phi(\tau)|\tau|^{\alpha_u+\omega}$ and k is a new scaling function which is derived from j and which depends on the choice of a_0.

As above, we take ω equal to unity. Further, if we assume $-\alpha_u$ to be accurately equal to unity,[8] corresponding to $\delta=2$, it follows that if we plot

$$\frac{(-\partial s/\partial T)_{P,x}(T,x)-(-\partial s/\partial T)_{P,x}(T,x_0)}{x-x_0}$$

versus $(x-x_t)/(T-T_t)$ for several values of T, we should expect to see curves of identical shape that are merely displaced vertically from one another. We show such plots in Fig. 11, where curves at four values of $T>T_t$ are plotted for the choice $x_0=x_t(\chi_0=0)$. The data used for these plots were obtained from least-squares fitting of closed algebraic forms to the data of Alvesalo, Berglund, Islander, Pickett, and Zimmermann[7] carried out by Dockendorf.[42] The range in T,x space covered by these plots is shown by the horizontal lines in the phase diagram of Fig. 1.

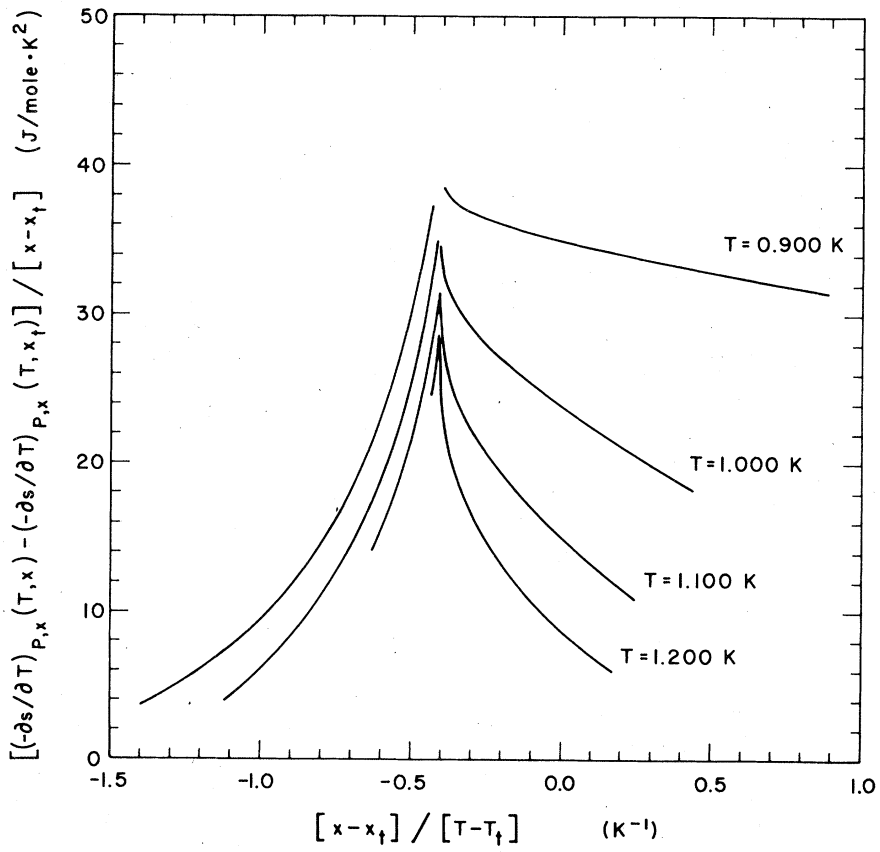

FIG. 11. Scaling plot derived from the specific heat results of ABIPZ (see Refs. 7 and 42) testing an implication of the RMB scaling form. (See Ref. 12.)

It will be seen that while the data in the superfluid region to the left of the λ anomaly appear to scale in this fashion, those to the right do not. The situation to the right would not be significantly changed if we were to alter the plot so as to allow $-\alpha_u$ to be 1.05, corresponding to $\delta = 2.05$.

VIII. $(\partial x/\partial\Delta)_{T,P}$ VERSUS T AT CONSTANT Δ

In considering questions of universality along the λ curve, one is interested in behavior at constant Δ rather than at constant x. In particular, it occurred to us that our observation in Sec. VI of somewhat larger values of $\alpha_\pm$ for $x = 0.644$ than for $x = 0.594$ at constant x might not reflect the situation at constant Δ. In this section we describe the process by which we have obtained $(\partial x/\partial\Delta)_{T,P}$ vs T at constant Δ near the λ transition from our data at constant x. This process makes only rather weak use of the scaling hypothesis of Sec. VII, and we believe that the results are not significantly influenced by this use.

Our procedure is illustrated in Fig. 12. The RMB scaling hypothesis specifies that $(\partial x/\partial\Delta)_{T,P}$ varies along curves of constant z in proportion to $|\chi|^{1-\delta}$. For $\omega = 1$, curves of constant z are simply straight lines in the T,x plane radiating from the tricritical point. Thus from our values of $(\partial x/\partial\Delta)_{T,P}$ vs T at constant x we may determine values at nearby points with simplicity and reasonable accuracy.

We determine the curve of constant $\Delta = \Delta_0$ which crosses the λ curve at the same point as the line of constant $x = x_0$ along which the data lie as follows. At any value of T near $T_\lambda(x_0) = T_{\lambda 0}$ we determine $\Delta_\lambda(T) - \Delta_0$ by means of the equation

$$\Delta_\lambda(T) - \Delta_0 \cong \left[\frac{d\Delta_\lambda}{dT}\right]_0 (T - T_{\lambda 0}) + \frac{1}{2}\left[\frac{d^2\Delta_\lambda}{dT^2}\right]_0 (T - T_{\lambda 0})^2 , \tag{26}$$

taking values for $(d\Delta_\lambda/dT)_0$ and $(d^2\Delta_\lambda/dT^2)_0$ from the work of Islander and Zimmermann.[8] Then we in-

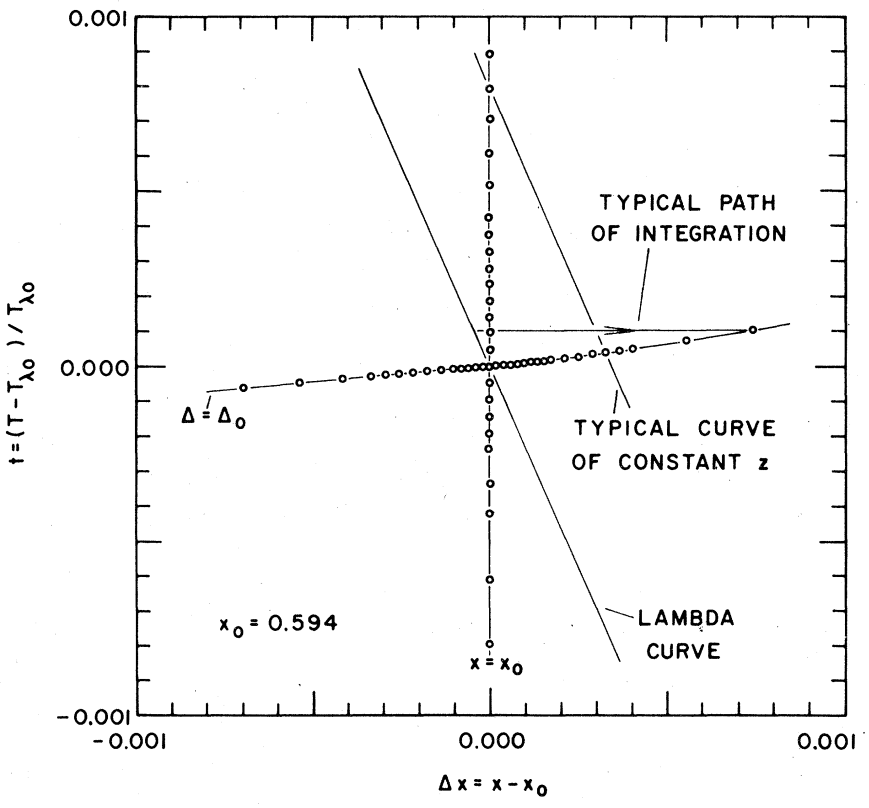

FIG. 12. Illustration of the construction of a path of constant Δ making use of data for $(\partial x/\partial\Delta)_{T,P}$ along a path of constant x, near the λ curve. The open circles show the data points recorded at constant $x = x_0$ and their counterparts at the same values of z along the curve of constant $\Delta = \Delta_0$. For a pair of points at a given value of z, note how much closer in temperature the point at constant Δ lies to the λ transition than the counterpart at constant x.

TABLE IV. Concentration susceptibility near the λ transition along curves of constant x and along curves of constant Δ.

$x_0 = 0.594$
$T_\lambda = 1.066\,550$ K
$(d\Delta/dT)_\lambda = -13.57$ J/(mole·K)
$(d^2\Delta/dT^2)_\lambda = -27.5$ J/(mole·K^2)

Constant $x = x_0$		Constant $\Delta = \Delta_0$		
$t = \frac{T - T_\lambda}{T_\lambda}$	$(\partial x/\partial\Delta)_{T,P}$ (J/mole)$^{-1}$	$t = \frac{T - T_\lambda}{T_\lambda}$	$(\partial x/\partial\Delta)_{T,P}$ (J/mole)$^{-1}$	$x - x_0$
0.009 798	0.301	0.000 733 6	0.316	0.003 750
0.007 173	0.327	0.000 511 0	0.339	0.002 793
0.004 454	0.363	0.000 292 8	0.371	0.001 769
0.003 235	0.391	0.000 200 9	0.397	0.001 298
0.002 391	0.422	0.000 140 8	0.427	0.000 967
0.001 828	0.446	0.000 103 0	0.449	0.000 743
0.001 360	0.477	0.000 073 2	0.480	0.000 556
0.000 984	0.499	0.000 050 4	0.501	0.000 404
0.000 891	0.505	0.000 044 9	0.506	0.000 366
0.000 797	0.519	0.000 039 5	0.521	0.000 328
0.000 703	0.529	0.000 034 1	0.530	0.000 290
0.000 609	0.541	0.000 028 9	0.542	0.000 251
0.000 516	0.561	0.000 023 8	0.562	0.000 213
0.000 422	0.578	0.000 018 9	0.579	0.000 175
0.000 375	0.585	0.000 016 5	0.586	0.000 155
0.000 328	0.592	0.000 014 1	0.593	0.000 136
0.000 281	0.603	0.000 011 8	0.604	0.000 117
0.000 234	0.615	0.000 009 5	0.615	0.000 097
0.000 188	0.646	0.000 007 2	0.646	0.000 078
0.000 141	0.685	0.000 005 1	0.685	0.000 058
0.000 094	0.778	0.000 003 2	0.778	0.000 039
0.000 047	0.913	0.000 001 5	0.913	0.000 019
0	0.964	0	0.963	0
−0.000 047	0.941	−0.000 001 5	0.941	−0.000 019
−0.000 094	0.927	−0.000 003 0	0.926	−0.000 039
−0.000 141	0.920	−0.000 004 5	0.919	−0.000 059
−0.000 188	0.906	−0.000 006 1	0.905	−0.000 079
−0.000 234	0.893	−0.000 007 6	0.891	−0.000 098
−0.000 328	0.866	−0.000 010 9	0.864	−0.000 138
−0.000 422	0.854	−0.000 014 2	0.851	−0.000 177
−0.000 516	0.848	−0.000 017 5	0.845	−0.000 217
−0.000 609	0.835	−0.000 020 9	0.832	−0.000 257
−0.000 703	0.823	−0.000 024 3	0.820	−0.000 296
−0.000 797	0.812	−0.000 027 8	0.808	−0.000 336
−0.000 984	0.800	−0.000 034 9	0.796	−0.000 415
−0.001 266	0.784	−0.000 045 8	0.778	−0.000 534
−0.001 641	0.773	−0.000 060 6	0.765	−0.000 694
−0.002 203	0.762	−0.000 083 4	0.753	−0.000 934
−0.002 860	0.747	−0.000 110 6	0.735	−0.001 215
−0.003 516	0.747	−0.000 138 4	0.732	−0.001 498
−0.004 829	0.727	−0.000 195 6	0.707	−0.002 070
−0.006 141	0.712	−0.000 255 5	0.688	−0.002 649
−0.008 017	0.698	−0.000 344 9	0.668	−0.003 490
−0.009 892	0.685	−0.000 438 9	0.648	−0.004 345

TABLE IV. (Cont'd.)

$x_0 = 0.644$
$T_\lambda = 0.944\,350$ K
$(d\Delta/dT)_\lambda = -10.70$ J/(mole·K)
$(d^2\Delta/dT^2)_\lambda = -19.5$ J/(mole·K^2)

Constant $x = x_0$		Constant $\Delta = \Delta_0$		
$t = \frac{T - T_\lambda}{T_\lambda}$	$(\partial x/\partial\Delta)_{T,P}$ (J/mole)$^{-1}$	$t = \frac{T - T_\lambda}{T_\lambda}$	$(\partial x/\partial\Delta)_{T,P}$ (J/mole)$^{-1}$	$x - x_0$
0.008 948	0.405	0.000 493 8	0.448	0.002 931
0.007 465	0.443	0.000 392 0	0.482	0.002 493
0.006 195	0.478	0.000 308 2	0.513	0.002 104
0.005 559	0.500	0.000 267 6	0.533	0.001 905
0.004 818	0.544	0.000 222 2	0.576	0.001 669
0.004 183	0.584	0.000 185 4	0.613	0.001 462
0.003 547	0.627	0.000 150 3	0.654	0.001 252
0.003 336	0.647	0.000 139 1	0.674	0.001 181
0.003 018	0.669	0.000 122 6	0.693	0.001 073
0.002 700	0.703	0.000 106 6	0.726	0.000 965
0.002 383	0.739	0.000 091 3	0.760	0.000 856
0.002 277	0.745	0.000 086 3	0.766	0.000 819
0.002 171	0.752	0.000 081 3	0.771	0.000 782
0.001 959	0.778	0.000 071 5	0.796	0.000 708
0.001 853	0.791	0.000 066 7	0.809	0.000 671
0.001 747	0.805	0.000 062 0	0.822	0.000 634
0.001 641	0.819	0.000 057 3	0.836	0.000 597
0.001 430	0.856	0.000 048 2	0.871	0.000 522
0.001 324	0.880	0.000 043 7	0.894	0.000 484
0.001 218	0.896	0.000 039 4	0.909	0.000 446
0.001 112	0.930	0.000 035 2	0.942	0.000 408
0.001 006	0.956	0.000 031 1	0.967	0.000 370
0.000 900	0.983	0.000 027 0	0.994	0.000 332
0.000 794	1.022	0.000 023 1	1.031	0.000 293
0.000 688	1.073	0.000 019 4	1.082	0.000 255
0.000 582	1.117	0.000 015 8	1.125	0.000 216
0.000 477	1.188	0.000 012 4	1.195	0.000 177
0.000 424	1.227	0.000 010 7	1.233	0.000 157
0.000 371	1.267	0.000 009 1	1.273	0.000 138
0.000 318	1.310	0.000 007 6	1.314	0.000 118
0.000 265	1.354	0.000 006 1	1.358	0.000 099
0.000 212	1.451	0.000 004 6	1.455	0.000 079
0.000 159	1.599	0.000 003 3	1.602	0.000 059
0.000 106	1.750	0.000 002 1	1.752	0.000 039
0.000 053	1.874	0.000 001 0	1.874	0.000 019
0	2.073	0	2.072	0
−0.000 053	2.238	−0.000 000 9	2.236	−0.000 020
−0.000 106	2.349	−0.000 001 8	2.345	−0.000 040
−0.000 159	2.428	−0.000 002 7	2.423	−0.000 060
−0.000 212	2.469	−0.000 003 5	2.462	−0.000 080
−0.000 265	2.428	−0.000 004 3	2.419	−0.000 100
−0.000 318	2.428	−0.000 005 2	2.418	−0.000 120
−0.000 371	2.388	−0.000 006 0	2.376	−0.000 140
−0.000 424	2.389	−0.000 006 9	2.375	−0.000 161
−0.000 477	2.350	−0.000 007 7	2.335	−0.000 181
−0.000 582	2.350	−0.000 009 5	2.332	−0.000 221
−0.000 709	2.275	−0.000 011 6	2.254	−0.000 270

TABLE IV. (Cont'd.)

$x_0 = 0.644$ (Cont'd.)

Constant $x = x_0$		Constant $\Delta = \Delta_0$		
$t = \frac{T - T_\lambda}{T_\lambda}$	$(\partial x/\partial\Delta)_{T,P}$ (J/mole)$^{-1}$	$t = \frac{T - T_\lambda}{T_\lambda}$	$(\partial x/\partial\Delta)_{T,P}$ (J/mole)$^{-1}$	$x - x_0$
−0.000 858	2.240	−0.000 014 2	2.215	−0.000 327
−0.001 006	2.205	−0.000 016 8	2.176	−0.000 385
−0.001 112	2.171	−0.000 018 7	2.140	−0.000 426
−0.001 218	2.171	−0.000 020 7	2.137	−0.000 467
−0.001 366	2.105	−0.000 023 4	2.069	−0.000 525
−0.001 483	2.105	−0.000 025 7	2.065	−0.000 570
−0.001 747	2.105	−0.000 030 7	2.058	−0.000 674
−0.001 959	2.074	−0.000 034 9	2.022	−0.000 758
−0.002 277	2.043	−0.000 041 2	1.984	−0.000 884
−0.002 488	2.013	−0.000 045 6	1.950	−0.000 968
−0.002 806	1.984	−0.000 052 2	1.914	−0.001 096
−0.003 018	1.984	−0.000 056 8	1.908	−0.001 182
−0.003 759	1.928	−0.000 073 1	1.837	−0.001 485
−0.004 395	1.928	−0.000 087 7	1.821	−0.001 750
−0.005 030	1.901	−0.000 102 8	1.781	−0.002 018
−0.005 665	1.875	−0.000 118 5	1.741	−0.002 291
−0.006 936	1.875	−0.000 151 2	1.711	−0.002 850
−0.008 207	1.875	−0.000 185 6	1.681	−0.003 428
−0.009 372	1.901	−0.000 218 4	1.678	−0.003 974

tegrate $(\partial x/\partial\Delta)_{T,P}^{-1}$ at constant T according to the relation

$$\Delta(T,x) - \Delta_0 = \Delta_\lambda(T) + \int_{x_\lambda(T)}^{x} \left(\frac{\partial x}{\partial \Delta}\right)_{T,P}^{-1} dx - \Delta_0 \qquad (27)$$

up to whatever value of x causes the right-hand side to vanish. We then have found the x coordinate of the curve $\Delta = \Delta_0$ at temperature T, and can then evaluate $(\partial x/\partial\Delta)_{T,P}$ there.

It proved possible to develop a simple search routine for carrying out this calculation which enabled direct integration of values of $(\partial x/\partial\Delta)_{T,P}^{-1}$ determined from our data without interpolation and which yielded values for $(\partial x/\partial\Delta)_{T,P}$ at Δ_0 for which z was the same as for the original points. Thus these calculated values were in one-to-one correspondence with the original values. Table IV lists these corresponding values of $(\partial x/\partial\Delta)_{T,P}$ together with their reduced temperatures relative to $T_{\lambda 0}$ and the corresponding values of $x(\Delta_0) - x_0$. Each row of Table IV corresponds to a particular value of z.

Plots of $(\partial x/\partial\Delta)_{T,P}$ at constant Δ vs $\ln|t|$ near the λ curve are shown in Fig. 13. Table IV is the source for both Fig. 13 and Fig. 8. It is interesting to note that the temperatures of the points in Fig. 13 are more than an order of magnitude closer to the λ transition than those of the corresponding points in Fig. 8, a situation which Fig. 12 provides help in understanding. However, the shapes of the plots in Fig. 13 are very similar to those in Fig. 8. While the plots for $x_0 = 0.594$ appear to be reasonably straight, the plot for $T > T_\lambda$ at $x_0 = 0.644$ appears to have a distinct upward curvature, which could conceivably be shared with the curve for $T < T_\lambda$ with a small shift in T_λ.

Thus the transformations that we have made from paths of constant x to paths of constant Δ fail to account for the departure from $\ln|t|$ behavior which we observe at $x = 0.644$ along a path of constant x. We note in passing that a transformation of this type is the (inverse of the) one considered by Fisher leading to exponent renormalization.[43] Ryschkewitsch and Meyer have carried out a similar transformation of their data for $x < x_t$ by a somewhat different technique.[16]

IX. CONCLUSIONS

In this work we have measured the temperature dependence of $(\partial x/\partial\Delta)_{T,P}$ at several values of x near the tricritical point by means of differential osmotic pressure measurements. In particular, we have studied the behavior of $(\partial x/\partial\Delta)_{T,P}$ near the λ transition

at two values of x and found pronounced peaks there. At constant x, for $3\times10^{-4}\lesssim|t|\lesssim10^{-2}$, these peaks may be characterized both above and below the transition by the form $(A_\pm/\alpha_\pm)(|t|^{-\alpha_\pm}-1)+B_\pm$ with exponents $\alpha_\pm$ lying in the range from ~0.0 to ~-0.2. At constant Δ, the peaks appear to be characterized by similar exponents.

According to the universality hypothesis, the exponents $\alpha_\pm$ describing the asymptotic behavior at constant Δ should be independent of position along the λ curve. Furthermore, these exponents should be the same as those describing the temperature dependence of $(\partial s/\partial T)_{P,\Delta}=c_{P,\Delta}/T$ along paths of constant Δ at the λ curve. This latter property

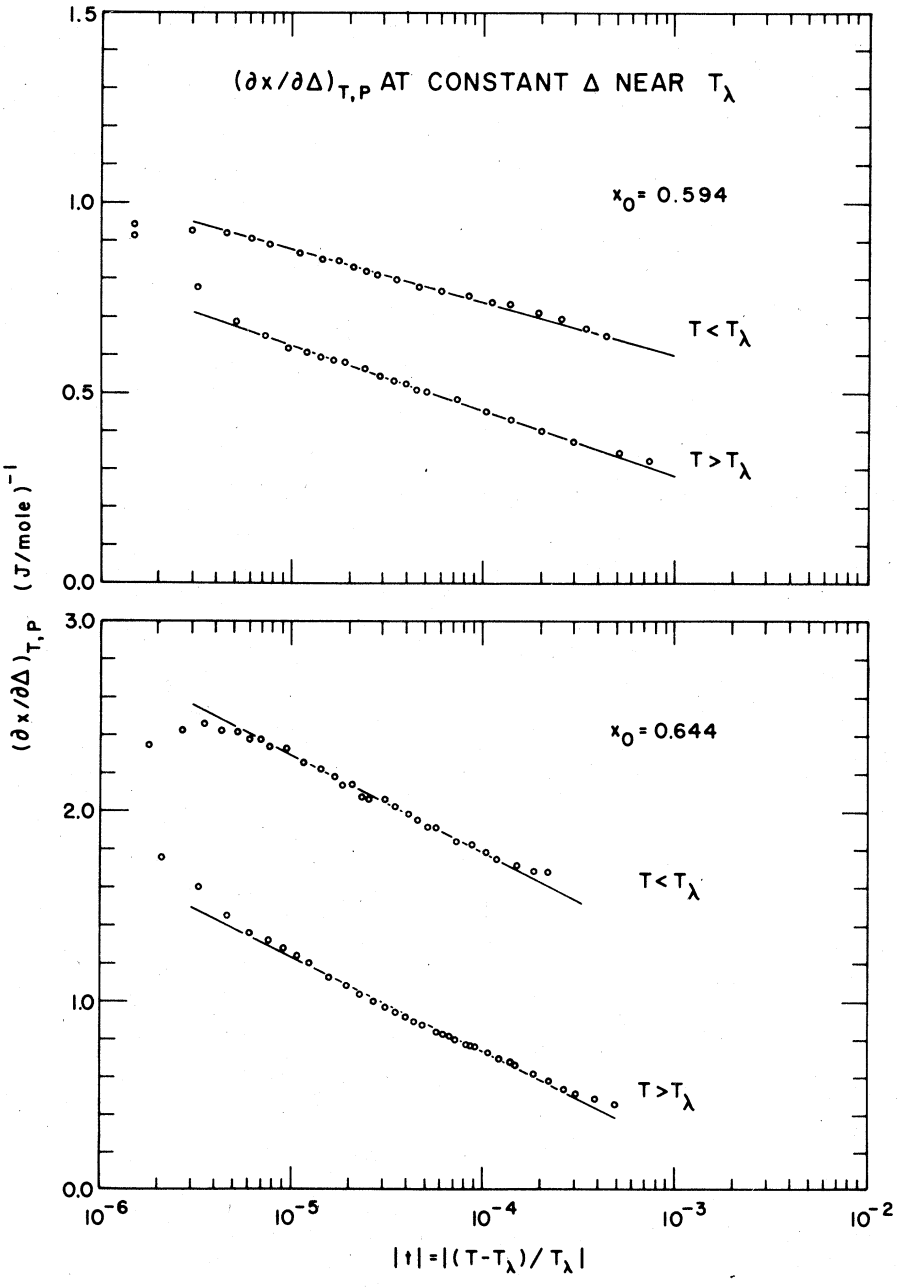

FIG. 13. Semilog plots of the concentration susceptibility vs the absolute value of the reduced temperature near the λ transition along paths of constant Δ. The values of x given are those at the λ curve. The lines are simply straight lines drawn to guide the eye.

may be obtained by use of the thermodynamic relationship

$$\left(\frac{\partial x}{\partial \Delta}\right)_{T,P} = \frac{\left(\frac{\partial s}{\partial T}\right)_{P,\Delta} - \left[\left(\frac{ds}{dT}\right)_{P,\lambda} - \left(\frac{d\Delta}{dT}\right)_{P,\lambda}\left(\frac{dx}{dT}\right)_{P,\lambda}\right]}{\left(\frac{d\Delta}{dT}\right)^2_{P,\lambda}}, \tag{28}$$

where the total derivatives are to be evaluated along curves at constant P parallel to the λ curve passing through the points in question.[8] The total derivatives will then all be finite and nonzero at the λ curve, and although they may still be singular there, their range of variation near the λ curve should be relatively small. Further, the quantity

$$(ds/dT)_{P,\lambda} - (d\Delta/dT)_{P,\lambda}(dx/dT)_{P,\lambda}$$

at the λ curve is quite small compared to our expectations for $(\partial s/\partial T)_{P,\Delta}$ near there, at our values of x.[8] Thus the asymptotic form of $(\partial x/\partial \Delta)_{T,P}$ should reflect well the asymptotic form of $(\partial s/\partial T)_{P,\Delta}$.

Gasparini and Gaeta[44] have shown that when provision is made for confluent singularity corrections to simple power-law critical behavior, the specific heat of Gasparini and Moldover[45] for mixtures with values of x up to 0.39 are consistent with $c_{P,\Delta}$ along paths of constant Δ having universal values of the leading exponents $\alpha_\pm$ equal to -0.022.

Our data at $x = 0.594$ appear to be consistent with their result without allowance for confluent singularities. The significance of our observation of $\alpha_\pm$ exponents somewhat greater than zero at $x = 0.644$ is not clear. If the effect is not of experimental origin, it is conceivable that tricritical crossover[46] is playing a role and that our measurements do not extend sufficiently close to the λ curve to see pure asymptotic λ behavior.

We have tested the RMB scaling hypothesis in the form

$$\left(\frac{\partial x}{\partial \Delta}\right)_{T,P} = f(x)\Xi^{-1}\left[\left(\frac{T-T_t}{T_t}\right)\Big/\left|\frac{x-x_t}{x_t}\right|\right], \tag{29}$$

where $f(x)$ is some function of x alone, against our data. Except for some sign of a discrepancy in the normal-fluid region for $x < x_t$ away from the λ curve, we have found reasonable agreement both for $x < x_t$, even quite close to the λ curve, and for $x > x_t$. The RMB hypothesis that $f(x) = |(x-x_t)/x_t|^{1-\delta}$ was not included in our test. However, when the scaling form for the specific heat $c_{P,x}$ implied by the complete RMB hypothesis was tested against specific-heat data, the data were found to scale in the superfluid region but not in the normal-fluid region.

ACKNOWLEDGMENTS

We wish to thank H. Meyer for many discussions of this work, for keeping us informed of related work in his laboratory, and for his comments on this manuscript. One of us (WZ) would like to thank E. Byckling for a germinal conversation at the start of this work. We are indebted to W. L. Gutheil for the original design of the cryostat and to O. V. Lounasmaa for the loan of the CG-1 thermometer. We wish to acknowledge the support of this work by the United States Energy Research and Development Administration under Contract No. EY-76-S-02-1569.

*Present address: Dept. of Phys., Concordia College, Moorhead, MN 56560.

[1]R. B. Griffiths, Phys. Rev. B 7, 545 (1973).
[2]E. H. Graf, D. M. Lee, and J. D. Reppy, Phys. Rev. Lett. 19, 417 (1967).
[3]H. A. Kierstead, J. Low Temp. Phys. 24, 497 (1976).
[4]P. Leiderer, D. R. Watts, and W. W. Webb, Phys. Rev. Lett. 33, 483 (1974).
[5]P. Leiderer, in *Quantum Fluids and Solids*, edited by S. B. Trickey, E. D. Adams, and J. W. Dufty (Plenum, New York, 1977), p. 351.
[6]P. Leiderer, H. Poisel, and M. Wanner, J. Low Temp. Phys. 28, 167 (1977).
[7]T. A. Alvesalo, P. M. Berglund, S. T. Islander, G. R. Pickett, and W. Zimmermann, Jr., Phys. Rev. A 4, 2354 (1971).
[8]S. T. Islander and W. Zimmermann, Jr., Phys. Rev. A 7, 188 (1973).
[9]G. Ahlers and D. S. Greywall, Phys. Rev. Lett. 29, 849 (1972).
[10]F. H. Wirth, Ph.D. Thesis (State University of New York at Stony Brook, 1978), available from University Microfilms International, Ann Arbor, Mich. 48106; F. H. Wirth and E. H. Graf (unpublished).
[11]G. Goellner, R. Behringer, and H. Meyer, J. Low Temp. Phys. 13, 113 (1973).
[12]E. K. Riedel, H. Meyer, and R. P. Behringer, J. Low Temp. Phys. 22, 369 (1976).
[13]D. R. Watts and W. W. Webb, in *Low Temperature Physics-LT13*, edited by K. D. Timmerhaus, W. J. O'Sullivan, and E. F. Hammel (Plenum, New York, 1974), Vol. 1, p. 581; D. R. Watts, Ph.D. Thesis (Cornell University, 1973) (unpublished).
[14]H. Dandache and A. Briggs, J. Low Temp. Phys. 29, 275 (1977).
[15]M. Ryschkewitsch, T. Doiron, M. Chan, and H. Meyer, Phys. Lett. A 64, 219 (1977).
[16]M. G. Ryschkewitsch and H. Meyer (unpublished).
[17]S. T. Islander and M. T. Loponen, Phys. Lett. A 51, 157 (1975).

[18]P. Leiderer, D. R. Nelson, D. R. Watts, and W. W. Webb, Phys. Rev. Lett. 34, 1080 (1975).
[19]D. Roe and H. Meyer, J. Low Temp. Phys. 28, 349 (1977).
[20]D. B. Roe, G. Ruppeiner, and H. Meyer, J. Low Temp. Phys. 27, 747 (1977).
[21]C. A. Gearhart, Jr., Ph.D. Thesis (University of Minnesota, 1977), available from University Microfilms International, Ann Arbor, Mich. 48106.
[22]OFHC Copper Felt, Huyck Metals Co., Milford, Conn. 06460.
[23]Vycor Code 7930 porous glass, Corning Glass Works, Corning, N.Y. 14830.
[24]Stycast 2850 GT, Emerson and Cuming, Inc., Canton, Mass. 02021.
[25]M. F. Wilson, D. O. Edwards, and J. T. Tough, Rev. Sci. Instrum. 39, 134 (1968).
[26]C. A. Gearhart, Jr. and W. Zimmermann, Jr., Phys. Lett. A 48, 49 (1974).
[27]See J. P. Romagnan, J. P. Laheurte, and H. Dandache, J. Phys. (Paris) 38, 59 (1977), for a recent reference on this subject and for references to earlier work.
[28]General Electric Co., Syracuse, N.Y. 13201.
[29]C. T. Van Degrift, Rev. Sci. Instrum. 46, 599 (1975).
[30]Model 5243L, Hewlett-Packard, Palo Alto, Calif. 94303.
[31]Model 580A, Hewlett-Packard, Palo Alto, Calif. 94303.
[32]Model 680, Hewlett-Packard, Palo Alto, Calif. 94303.
[33]F. G. Brickwedde, H. van Dijk, M. Durieux, J. R. Clement, and J. K. Logan, J. Res. Natl. Bur. Stand. Sect. A 64, 1 (1960).
[34]S. G. Sydoriak and T. R. Roberts, Phys. Rev. 118, 901 (1960).
[35]R. H. Sherman, S. G. Sydoriak, and T. R. Roberts, J. Res. Natl. Bur. Stand. Sect. A 68, 579 (1964).
[36]Cryocal, Inc., Minneapolis, Minn. 55435.
[37]Andonian Cryogenics, Inc., Newtonville, Mass. 02160.
[38]Cat. No. RBR-55L-40001-FP, 40 k Ω, Ultronix, Inc., Grand Junction, Colo. 81501.
[39]C. A. Gearhart, Jr., J. A. McLinn, and W. Zimmermann, Jr., Rev. Sci. Instrum. 46, 1493 (1975).
[40]E. C. Kerr, Phys. Rev. Lett. 12, 185 (1964), and private communication.
[41]N. Giordano and W. P. Wolf, in *Magnetism and Magnetic Materials—1975,* edited by J. J. Becker, G. H. Lander, and J. J. Rhyne (AIP., New York, 1976), p. 459.
[42]L. D. Dockendorf, M.S. Thesis (Univeristy of Minnesota, 1974) (unpublished).
[43]M. E. Fisher, Phys. Rev. 176, 257 (1968); see also M. E. Fisher and P. E. Scesney, Phys. Rev. A 2, 825 (1970).
[44]F. M. Gasparini and A. A. Gaeta, Phys. Rev. B 17, 1466 (1978).
[45]F. M. Gasparini and M. R. Moldover, Phys. Rev. B 12, 93 (1975).
[46]E. K. Riedel and F. J. Wegner, Phys. Rev. B 9, 294 (1974).